The Anatomical Record

A Cross-Species Comparison of Metabolite Profiles in Chemosensory Epithelia: an indication of metabolite roles in chemosensory cells

Journal:	*Anatomical Record*
Manuscript ID:	AR-07-0164.R1
Wiley - Manuscript type:	Full Length Article
Date Submitted by the Author:	n/a
Complete List of Authors:	Mobley, Arie; University of Utah, Physiology Lucero, Mary; University of Utah, Physiology Michel, William; University of Utah, Physiology
Keywords:	Olfactory, Vomeronasal, Mouse, Zebrafish, Squid

Title: A Cross-Species Comparison of Metabolite Profiles in Chemosensory Epithelia: an indication of metabolite roles in chemosensory cells

Authors:

Arie Sitthichai Mobley[1], Mary T. Lucero[1], William C. Michel[1]
Department of Physiology
University of Utah
420 Chipeta Way, Ste. 1700
Salt Lake City, UT 84108-6500

Corresponding author:

Arie Sitthichai Mobley
Department of Physiology
University of Utah
420 Chipeta Way, Ste. 1700
Salt Lake City, UT 84108-6500
arieann13@yahoo.com
phone: 203-464-2369
fax: 203-785-4361

Running title: Cross-Species Comparison of Metabolite Profiles

Associate Editor: Kurt Albertine, University of Utah

Keywords: Olfactory, Vomeronasal, Mouse, Zebrafish, Lobster, Squid

Abbreviations: AOI, area of interest; Arg, arginine; Asp, aspartate; ATG, aesthetasc tegumental glands; EC, ensheathing cell; Glu, glutamate; GSH, glutathione; Gly, glycine; IR, immunoreactivity; NOS, nitric oxide synthase; OE, olfactory epithelium; ORN, olfactory receptor neuron; RGB, red, green, blue; SC, sustentacular cell; Tau, taurine; VN, vomeronasal neuron; VNO, vomeronasal organ

Grant Sponsor: NIH NINDS; Grant number: DC006793-01 to A.S.M. and Grant number: P01 NS017938 to W.C.M. and M.T.L.

UU IR Author Manuscript

Abstract

Comparative studies of chemosensory systems in vertebrates and invertebrates have greatly enhanced our understanding of anatomical and physiological constraints of chemical detection. Immunohistochemical comparisons of chemosensory systems are difficult to make across species due to limited cross-reactivity of mammalian-based antibodies. Immunostaining chemosensory tissues with glutaraldehyde-based antibodies generated against small metabolites in combination with hierarchical cluster analyses provide a novel approach for identifying and classifying cell types regardless of species. We used this 'metabolite profiling' technique to determine whether metabolite profiles can be used to identify cell classes within and across different species including mouse, zebrafish, lobster and squid. Within a species, metabolite profiles for distinct cell classes were generally consistent. We found several metabolite-based cell classifications that mirrored function or receptor protein based classifications. Although profiles of all six metabolites differed across species, we found that specific metabolites were associated with certain cell types. For example, elevated levels of glutathione were characteristic of non-sensory cells from vertebrates, suggesting an anti-oxidative role in non-neuronal cells in sensory tissues. Collectively, we found significantly different metabolite profiles for distinct cell populations in chemosensory tissue within all of the species studied. Based on their roles in other systems or cells, we discuss the roles of L-arginine, L-aspartate, L-glutamate, glycine, glutathione, and taurine within chemosensory epithelia.

Introduction

Across species of vertebrates and invertebrates, chemosensory systems have several common features. In general, olfactory receptor neurons (ORNs) are primary sensory neurons, with odorant-specific signal transduction machinery localized to cilia or microvilli on apical dendrites, and basal unmyelinated axons projecting to a glomerular structure in the brain (Ache,

1994). Basic properties of odorant receptors, and signal transduction strategies show more similarities than differences among species as diverse as rodents, birds, fish and insects (Eisthen, 2002). However, the limitations associated with species-specific antibodies have precluded an across-species, functional comparison of cell types within olfactory epithelia.

Free amino acids and other small metabolites such as glutathione form unique antigens when conjugated to bovine serum albumin with glutaraldehyde during fixation (Steinbusch et al., 1978;Steinbusch et al., 1982). Antibodies generated against these antigens allow semi-quantitative measurements of small metabolite levels within cells. We can identify classes of cells by measuring the steady state levels of combinations of small metabolites. This metabolite profiling technique bypasses the need to identify unique proteins expressed in each cell type and provides antibody probes that are consistent when used in widely different species. Recent studies in visual and taste systems have shown that sensory cell types can be classified and identified across species by measuring levels of these small metabolic markers (Marc et al., 1995;Kalloniatis et al., 1996;Michel et al., 1999;Eram and Michel, 2005). Further, retinal signatures in a single species were used to show how the retina is remodeled during degeneration (Jones et al., 2003), emphasizing the importance of examining metabolite profiles in healthy tissue.

Mouse, zebrafish and lobster are well-established models for studying olfaction and represent vertebrates and invertebrates from terrestrial and aquatic environments (both marine and freshwater). Much is known about the anatomy and physiology of chemosensory systems in each model (Korsching et al., 1997;Koehl et al., 2001;Orlando, 2001;Steullet et al., 2002;Zufall et al., 2002;Beauchamp and Yamazaki, 2003;Trinh and Storm, 2004). We used antibodies that recognize the following glutaraldehyde-conjugated antigen complexes: L-arginine, L-aspartate, L-glutamate, glycine, glutathione, or taurine. We examined the expression of these metabolites

in cells of the mouse olfactory epithelium (OE), zebrafish OE, lobster olfactory antennules, and in the mouse vomeronasal organ (VNO). In addition, we applied the same analyses to the less-characterized squid OE. We include mouse VNO in our study to look at whether zebrafish microvillar cells have similar metabolite profiles to mouse vomeronasal neurons. While a metabolite profile comparison of gustatory and olfactory systems may be interesting, it is outside the scope of this study.

The markers were chosen to separate functionally different cell populations, while providing information regarding the metabolism of these cells. For example, glutathione should be highest in cells that generate and remove reactive oxygen species such as support cells (Hayes and McLellan, 1999;Bringmann et al., 2006). Taurine is often used by cells that must cope with large osmotic challenges (Pierce, 1982;Lambert, 2004). Arginine is important in cells either undergoing proliferation (Rodriguez et al., 2007) or undergoing stress (Tong and Barbul, 2004;Wheatley, 2005) and is a precursor for nitric oxide signaling (Mayer et al., 1991). Glutamate is a core metabolite in all cells, an indicator of the health or activity of cells, as well as a neurotransmitter (Takeuchi, 1987;Gasic and Heinemann, 1991;Hertz and Peng, 1992;Di Giorgi Gerevini et al., 2004;Torres and Amara, 2007), specifically in vertebrate ORNs (Trombley and Shepherd, 1993). Free aspartate is primarily used as a glutamate precursor (Palaiologos et al., 1989).

Biochemical studies have ascertained the amino acid content in olfactory epithelium and bulb in various species to evaluate a metabolite's significance (Watanabe et al., 1990;Potter et al., 1995;Ebbesson et al., 1996;Miranda-Contreras et al., 2000). These studies do not identify the metabolite content within cell types of the olfactory epithelium or bulb. Our approach provides a snapshot of the metabolic profile of each cell within a section of tissue. Similarities and differences of free metabolite levels within cells of chemosensory epithelia across vertebrate or

invertebrate species allow us to generate testable models of functional similarities and differences between cells, epithelia and species.

To determine whether the extensive consistency in certain markers within retinal cell types across species (Marc et al., 1995;Kalloniatis et al., 1996;Marc et al., 1998;Marc and Cameron, 2001;Marc and Jones, 2002) is also found in chemosensory systems, we asked the following three questions: 1) Are metabolite profiles for functionally distinct cell types consistent across animals *within* a species? 2) Are metabolite profiles for analogous cell types conserved *across* species? 3) Will a comparative study of metabolite profiles in the three model organisms inform us about metabolite roles in the less studied squid olfactory organ?

Methods

Animals

Mice

Adult Swiss-Webster mice (n = 3; 18-20 g, Charles River Laboratory, Wilmington, MA, USA) were deeply anesthetized with 2.5 µl/g sodium phenobarbitol, fixed by perfusion with 1% paraformaldehyde/2.5% glutaraldehyde, and decapitated. After removing the skin and lower jaw, the head was post-fixed overnight at 4°C followed by decalcifier (Apex Engineering Products Corp., Plainfield, IL) for 3 hours at room temperature. The overlying bone was removed and intact olfactory and vomeronasal tissues were rinsed and stored in 0.1 M PBS at 4°C overnight, dehydrated using a methanol and acetone series, and embedded in Eponate plastic (65% DDSA, 33% Eponate, 2% DMP-30, allfrom Ted Pella Co., Redding, CA). All chemicals are from Sigma-Aldrich Corp. (St. Louis, MO) unless stated otherwise. All animal procedures were approved by the University of Utah Institutional Animal Care and Use Committee.

Zebrafish

Adult zebrafish, *Danio rerio* (n = 3; total body length 2.8 -3.3 cm) were purchased from a commercial supplier, and housed at the University of Utah in a recirculating 40-80 L aquaria (26°C). Animals were fed flake food (TetraMin, Blacksburg, VA) daily until used. Fish were anesthetized with MS-222 (20 mg/l in artificial freshwater), decapitated, and the head was immersed in 1% paraformaldehyde/2.5% glutaraldehyde overnight at 4°C. Olfactory rosettes were removed, and then rinsed in 0.1 M PBS, dehydrated and embedded in plastic.

Lobster

Live Caribbean spiny lobsters, *Panulirus argus* (n = 3; 45-80 mm carapace length) were caught in the Florida Keys and air freighted to Georgia State University in care of Dr. Charles D. Derby. The lobsters were held in an 800 L recirculating aquarium containing aerated Instant Ocean (20-25°C) and fed frozen shrimp and squid until used. Each lateral flagellum of the antennule was removed, cut into pieces and placed in 1% paraformaldehyde/2.5% glutaraldehyde at 4°C overnight. Fixed tissue was shipped to W.C.M. for subsequent processing (0.1 M PBS rinse, dehydration and plastic embedding).

Squid

Live juvenile squid, *Lolliguncula brevis*, (n = 3; ~10 cm in length) were caught in the wild by the National Resource Center for Cephalopods (University of Texas Marine Biomedical Center in Galveston, TX) and shipped overnight. Immediately upon arrival, animals were decapitated, olfactory organs were dissected and pinned out on Sylgard©-coated coverslips and placed in 1% paraformaldehyde/2.5% glutaraldehyde at 4°C overnight. Fixed tissue was rinsed in 0.1 M PBS, dehydrated and embedded in plastic.

Tissue Processing

Olfactory and vomeronasal tissues were cut into consecutive 50-100 nm sections and collected on Teflon-coated 12-well spot slides (Erie Scientific Co., Portsmouth, NH). The

sections were further processed as reported by Marc et al. (1990). Briefly, sections were deplasticized with 25% sodium ethoxide (saturated sodium hydroxide in absolute ethanol) for 7 min, followed by three 2 min rinses in 100% methanol, then double distilled H_2O for 5 min. Individual sections were stained with one of the following rabbit polyclonal primary antibodies (final dilution): anti-arginine (1:500), anti- aspartate (1:2000), anti-glutamate (1:32000), anti-glycine (1:4000) or anti-glutathione (1:4000), and anti-taurine (1:16000) (Signature Immunologics, Salt Lake City, UT) overnight at room temperature. Primary antibodies were diluted in 0.1 M PBS containing 1% goat serum and 0.05% thimerosal (pH 7.4). It is not possible to do Western blots with these antibodies because they only recognize glutaraldehyde-conjugated haptens. Dot blot analysis performed by Marc et al. (1990, 1995) indicates that the aspartate, glutamate, glycine, taurine (Marc et al., 1990) and arginine (Marc et al., 1995) antibodies are at least 1,000-fold less cross-reactive to other structurally related antigens. Low cross-reactivity for glutathione (<1:1000) is reported by the manufacturer (Signature Immunologics, Inc., SLC, UT). Elimination of any of the primary antibodies from the procedure resulted in no immunoreactivity (Fig. S1). Secondary nanogold-conjugated goat anti- rabbit antibodies (1:50 dilution; Amersham Corp., Arlington Heights, IL, USA) were applied for one hour and visualized with silver intensification (0.14% silver nitrate, 43 mM hydroquinone, 64 mM citric acid, 141 mM sodium citrate) for 3 min at 32°C. Slides were coverslipped with Eponate plastic and cured at 65°C. All experiments were performed in triplicate.

Imaging and Analysis

For each animal, we acquired sets of six images of serial sections; each section stained with one of the six antibodies. Each 8-bit grayscale image was captured with an Axiocam CCD camera at 40X on a Zeiss upright Axioplan2 microscope. One image was selected as the reference and the other five images were registered to that image using PCI Geomatica 8.0 (PCI

Remote Sensing, Richmond Hill, Ontario, Canada). Images at higher magnification were captured at 63X. Although similar exposure times and light levels were used during image capture, small differences in background intensities were measured from a region without tissue and used to set equivalent levels across allimages within a species. Two sets of superimposed red, green, blue (RGB) images were made in Adobe Photoshop 6.0 (Adobe, San Jose, CA) by placing images of taurine or arginine immunoreactivity (IR) in the red channel, glutamate or aspartate IR in the green channel, and glutathione or glycine IR in the blue channel, respectively. To select areas of interest (AOI) for an RGB image set, we used Image Pro Plus (MediaCybernetics, Silver Spring, MD). AOIs were placed on individual cells or features of the tissue on RGB images. AOI placements were saved and applied to each registered image in that set to obtain pixel intensity measurements for allAOI s. All AOIs were examined in both RGB images to confirm that borders remained within a single cell or feature. For each species, the AOIs from the image sets were grouped and classified using hierarchical cluster analysis based on differences in pixel intensity (SPSS 14.0, SPSS Inc., Chicago, IL). Dendrograms from SPSS were reproduced for publication using Adobe Illustrator CS (Adobe, San Jose, CA). Multivariate analysis of variance (MANOVA; post-hoc test, $p<0.05$) was used to determine the number of significantly different classes for a given tissue; at least one of all possible pairwise comparisons of pixel intensity measurement was significantly different. Histograms of the mean ± S.D. pixel intensity from each class were made in Origin 6.0 (OriginLab, Northampton, MA). After all AOIs had been classified within a given species, the mean ± S.D. pixel intensities from all classes across all tissues were subjected to hierarchical cluster analysis. MANOVAs were used to determine the number of significantly different classes across all tissues. Throughout the text, the pixel intensity ranges of metabolite labeling are described as follows: 0-85 = low; 86-140 = medium; 141-199 = high; 200-255 = very high.

Results

The levels of six metabolites were analyzed immunohistochemically in the olfactory epithelium (OE) of mouse, zebrafish and squid, the mouse VNO and lateral flagellum of the lobster antennule. The results first describe the immunohistochemistry and classification of each species' chemosensory tissue followed by a comparison of the metabolite profile based classes across species.

Immunohistochemistry of mouse OE

The pseudostratified mouse OE consists of ORNs (mature and immature), sustentacular cells (SCs), microvillar cells, horizontal and globose basal progenitor cells (Fig. 1). A lamina propria beneath the OE contains connective tissue, olfactory axon bundles surrounded by olfactory ensheathing cells (ECs), extrinsic nerve bundles, glands and blood vessels (Fig. 1A). The transition from OE to respiratory epithelium (RE) was revealed by changes in the pattern of aspartate (Fig. 1B), glutamate (Fig. 1C), glycine (Fig. 1D), glutathione (Fig. 1E) and taurine (Fig. 1F) immunoreactivity (IR). Two cells within the respiratory epitheliumwere distinguished by their high aspartate, glutamate, and glutathione levels (Fig. 1, yellow AOIs).

In the mouse OE, arginine labeling was low (Fig. 1A) except for in the olfactory ECs (Fig. 1A, green AOI). Aspartate IR was heterogeneous; highest labeling was observed in the basal layer, intermediate labeling in the apical region and lowest labeling in the ORN cell bodies in the middle layer (Fig. 1B, H). Glutamate and glutathione labeling was also heterogeneous with higher labeling in the apical SCs and basal OE than in the ORN cell bodies (Fig. 1C, E, G). ORN cell bodies only showed high labeling for taurine (Fig. 1F, G). In an RGB image of taurine, glutamate and glutathione most ORNs appeared orange due to high taurine and medium glutamate labeling (Fig. 1G, I). Three glutamate positive ORNs were found in the apical OE (Fig. 1A, orange AOIs, Fig. 1C, G, I, arrowhead). Thus, mature ORNs in the middle third of the

OE had relatively lower metabolite levels than the rest of the OE. With respect to overall intensity, taurine > glutathione > aspartate > glutamate > glycine > arginine.

Mouse OE has nine metabolically distinct cell classes.

The hierarchical clustering of all AOIs in the mouse OE from three animals is shown in Figure 2A. Using MANOVA ($p < 0.05$) to compare six metabolites in mouse OE, we found nine significantly different classes of cells. Classes 4, 5 and 7 were found in all three animals. Classes 1, 8 and 9 consisted of AOIs from two animals. Classes 2, 3 and 6 contained AOIs placed on non-sensory regions in one animal. The initial branching of the dendrogram generated by hierarchical cluster analysis separated Class 1, with low levels of all metabolites, from the other classes. Class 1 contained connective tissue present in the lamina propria (Fig. 1 A, blue AOIs). The next branching of the dendrogram separated Classes 2 and 3 from Classes 4-9 based on glutathione and glutamate levels. Classes 2 and 3 were significantly different from each other based on aspartate and taurine levels (Fig. 2F). Class 2 consisted of distinct respiratory cells (Fig. 1A, yellow AOIs, Fig. 1B, H, arrowhead). Class 3 metabolites defined the Bowman's glands (Fig. S2). Class 4 identified olfactory ECs, the only cells in the mouse OE with significant arginine content (Fig. 1A, green AOI, Fig. 1H, arrow). Class 5 consisted of AOIs that were present in the middle, or ORN, layer of the OE, and were separated from the remaining Classes 6-9 by significantly lower glutathione levels (Fig. 1A, cyan AOIs). Class 6 respiratory cells were distinguished from Classes 7-9 by high glycine levels (Fig. 1A, magenta AOIs, Fig. 1D, H, arrow). Class 7 consisted of cells located in the apical and basal layers of the OE, and was distinguished from Classes 8 and 9 by lower aspartate levels (Fig. 1A, purple AOIs). Finally, Classes 8 and 9 had significantly different glutamate levels. Class 8 AOIs identified ducts of the Bowman's glands (data not shown, but see Fig. S2B). Class 9 consisted of a class of apical ORNs that were high in glutamate (Fig. 1A, orange AOIs, Fig. 1C, G, I, arrowhead).

Thus, hierarchical cluster analysis confirmed that different cell types in the mouse OE have unique metabolite profiles, the majority of which are conserved across preparations.

Immunohistochemistry of themouse VNO

The mouse VNO is located near the anterior base of the nasal septum. The pseudostratified VNO epithelium can be divided into thirds with the apical third containing sustentacular cell (SC) bodies (Martinez-Marcos et al., 2005), the middle third containing $G\alpha_{i2}$-expressing apical vomeronasal neurons (VNs), and the basal third containing $G\alpha_{o}$-expressing basal VNs (Jia and Halpern, 1996;Menco et al., 2001). There was very little arginine labeling in any cell type of the VNO, (Fig. 3A) however, the ensheathing cellswhich wrap VN axons had high arginine IR (Fig. S3). Medium aspartate labeling was observed in both the VNs and SCs (Fig. 3B). Glutamate IR was higher in the VNs than the SCs (Fig.3C). Glycine labeling distinguished the basal VNs from apical VNs and the SCs (Fig. 3D). Glutathione labeling was high in the SCs of the VNO, compared to the VNs (Fig. 3E). Although taurine was in the high range for VNs and SCs, the relative distribution for taurine was SCs > apical VNs > basal VNs (Fig. 3F and 4B). In an RGB image of taurine, glutamate and glutathione, the basal VNs appeared green (glutamate), while the apical VNs appeared yellow due to the higher levels of taurine (Fig. 3G, I). In an RGB image of arginine, aspartate and glycine (Fig. 3H), the basal VNs were blue due to higher glycine labeling. In summary, glycine and taurine delimited the apical and basal VNs, while glutamate and glutathione distinguished the SCs from the VNs. Labeling intensity overall varied depending on the cell type, however glutamate, glutathione and taurine had greater intensity than arginine, aspartate and glycine.

Mouse VNO has 12 metabolically distinct cell classes.

The hierarchical clustering of all AOIs in the mouse VNO from three animals is shown in Figure 4A. Using MANOVA ($p < 0.05$) to compare six metabolites in mouse VNO, we found

12 significantly different classes of cells. Classes 1, 2, 4, and 5 were found in all three animals. Classes 6 and 10 consisted of AOIs from two animals. Classes 3, 7, 8, 11 and 12 were comprised of rare cells or non-sensory regions from one animal. The first branch of the VNO dendrogram separated the VNs, SCs and ensheathing cells (Classes 1-9) from the remaining non-sensory cell types (Classes 10-12; Fig. 4). The Class 9 ensheathing cells were split from Classes 1-8 because of their high arginine content (Fig. S3, orange AOIs). Classes 7 and 8 were separated from Classes 1-6 based on higher aspartate levels. Classes 7 and 8 each contained one AOI and were separated by relative arginine, glutamate and glutathione labeling (Fig. 3A, peach AOI, Fig. 3B, H, arrowhead). Classes 1-6 split into two groups with Classes 1-4 having significantly lower glutathione levels than Classes 5 and 6. The SCs in Classes 5 and 6 were separated on the basis of taurine differences (Fig. 3A, cyan and magenta AOIs). Classes 1-4 consisted of VNs. The basal VNs in Class 4 had significantly lower taurine levels (Fig. 3A, green AOIs, Fig. 3F, G, I, arrowhead) than Classes 1-3. Classes 1 (Fig. 3A, blue AOIs, Fig. 3E, arrow) and 3 (Fig. S3, red AOIs) consisted of the apical VNs, which were distinguished by glutathione and taurine levels. The Class 2 basal VNs differed from Classes 1 and 3 based on significantly elevated arginine labeling (Fig. 3A, yellow AOIs, Fig. 3E, arrow). The non-sensory cell types in Classes 10-12 included connective tissue in Class 10 with higher glutamate and glutathione levels (Fig. 3A, cream AOI, Fig. 3C, E, G, I, arrow). Class 11 glands (Fig. 3A, pink AOIs, Fig. 3F, G, arrow) had higher taurine content than blood vessels in Class 12 (Fig. 3A, maroon AOIs, Fig. 3F,G, arrow) (Mendoza, 1993). Thus, across animals, VNs and SCs are more similar to each other than to the other cell types (glands and connective tissue), as illustrated by the dendrogram and histograms in Fig. 4A-B.

Immunohistochemistry of zebrafish OE

The OE of the zebrafish, *Danio rerio*, is present on olfactory lamellae, with sensory epithelium covering approximately the inner two thirds and non-sensory epithelium (NSE) covering the outer third (Fig. 5). The metabolite profile of the zebrafish OE is similar to the mouse OE in that there was very low arginine IR but high levels of glutamate and taurine (Fig. 5A, C, F). Medium aspartate IR was present in a subset of cells in both the OE and the NSE (Fig. 5B). A subset of ORNs had medium glutamate IR compared to other cells in the OE or NSE (Fig. 5C, arrow). The zebrafish OE and NSE had high levels of glycine labeling, with a basal layer of cells showing the highest glycine IR (Fig. 5D, arrow). Glutathione labeled the apical layer of the OE as well as the NSE (Fig. 5E). Medium levels of taurine labeling were observed in the majority of ORNs and medium to low labeling in NSE areas. An RGB image of taurine, glutamate and glutathione (Fig. 5G, I), revealed the three main types of cells in the OE. There were basal ORNs that spanned the width of the OE (Fig. 5A, yellow AOIs, Fig. 5C, G, I, large arrow), apical ORNs (Fig. 5A, blue AOIs, Fig. 5C, G, I, small arrow), and basal cells (Fig. 5A, green AOIs). In the same RGB image, there were two types of cells in the NSE, with one type having higher taurine (Fig. 5A, red AOI) than the other (Fig. 5A, cyan AOIs). An RGB image of arginine, aspartate and glycine was mostly blue due to high glycine levels and low arginine or aspartate (Fig. 5H). Overall, the relative amounts of metabolites across the OE were glycine = glutamate = taurine > glutathione > aspartate > arginine labeling.

Five of eight zebrafish classes are non-sensory

Although zebrafish have 3 morphologically distinct types of ORNs (ciliated, microvillar and crypt cells) (Hansen and Zeiske, 1998) hierarchical analysis of all AOIs in the OE from three animals identified only two classes of ORNs (classes 1 and 2) in the sensory epithelia (Fig. 6). Classes 1, 2, 3, and 7 were found in all three animals. Classes 4, 5, 6 were found in one of two animals. Class 8 was found in one animal and identified non-sensory tissue at the base of the OE

with the highest glutathione labeling (Fig. S4, peach AOI). Classes3 and 5 through 8 were all NSE. Classes 6 and 7 were different from Classes 1-5 because of aspartate, glutamate and glutathione levels. Class 6 (Fig. S4, magenta AOIs) and Class 7 cells (Fig. 5A, purple AOI, Fig. 5C, G, arrowhead) were found in the basal lamina and other non-sensory tissue of the zebrafish OE. Class 6 was separated from Class 7 by its low aspartate and glutamate levels. Classes 3-5 were separated from Classes 1 and 2 primarily based on low taurine. Classes 5 (Fig. 5A, cyan AOIs, Fig. 5E, G; arrow) and 4 consisted of non-sensory cells and basal cells, respectively, and were distinguished by differences in glutathione levels. Class 4 cells had low glutathione and high glycine levels and were designated basal cells due to their proximity to the basement membrane (Fig. 5A, green AOIs, Fig. 4D, H; arrow). Class 3 NSE was distinguished from Classes 4 and 5 by low aspartate levels (Fig. 5A, red AOI, Fig. 5B, H; arrowhead). Finally, in Class 1 apical ORNs (Fig. 5A, blue AOIs, Fig. 5C, G, I; arrow) the aspartate, glutamate, glycine, glutathione and taurine levels were higher than Class 2 basal ORNs (Fig. 5A, yellow AOIs, Fig. 5C, G, I; arrow). In summary, the zebrafish OE had metabolite profiles similar to the mouse OE and VNO except for the high glycine levels in zebrafish OE.

Immunohistochemistry of lobster antennules

The distal half of the lateral flagellum of the first antennae of the lobster is divided into repeating units called annuli (Laverack, 1964;Ache and Derby, 1985). Each annulus has two rows of olfactory sensilla, called aesthetascs. Each aesthetasc is innervated by the outer dendritic segments of approximately 300 ORNs (Grünert and Ache, 1988). The ORN cell bodies associated with each aesthetasc are clustered within the lumen of the annulus (Fig. 7). Unlike the vertebrates we examined, cell bodies within lobster annuli had notably high arginine labeling (Fig. 7A). Aspartate, glycine and an absence of taurine clearly distinguished the ORNs from the surrounding tissue (Fig. 7B, D, F). Glutathione levels in the lobster were not as striking between

the ORNs and non-sensory epithelia (connective tissue, auxiliary cells and secretory rosettes), compared to the vertebrates (Fig. 7E). Taurine was absent from the majority of ORNs, but outlined the cell bodies as described previously (Steullet et al., 2000) (Fig. 7F). In subsets of ORNs, taurine varied between medium (Fig. 7F, arrowhead) and very high (Fig. 7F, arrow). In an RGB image containing taurine, glutamate and glutathione (Fig. 7G, I), the majority of ORNs are bright green compared to the surrounding auxiliary cells. The intense green color is due to high glutamate levels, while the yellow color in non-sensory tissue and a subset of ORNs is due to high levels of taurine. Thus, aspartate and glycine were high in lobster ORNs but were lower in surrounding tissue. Arginine and glutamate had the highest intensity in auxiliary cells and connective tissue, while glutathione had the lowest intensity overall.

Lobster antennules contain three classes of ORNs based on taurine

Seven classes of cells were identified in lobster olfactory tissue (Fig. 8). Classes 1, 2, and 6 were found in all three animals. Classes 4 and 7 were from two animals. Classes 3 and 5 were each found in one animal. The cluster analysis of all AOIs from three animals indicated that Class 7 cells were the most distinct. The Class 7 secretory cells of the aesthetasc tegumental glands (ATGs), called secretory rosettes, had very low levels of all the metabolites (Fig. 7A, purple AOIs, Fig. 7E, G). ATGs are a recently identified tissue component of lobster antennules (Schmidt et al., 2006). The remaining 6 classes of cells were divided into two groups (Classes 1-3 and Classes 4-6) on the dendrogram based on arginine, aspartate and taurine immunoreactivity. Class 3 (Fig. S5) had lower glycine levels than Classes 1 and 2. Differences in arginine and taurine labeling separated Classes 1 and 2 (Fig. 7A, blue and yellow AOIs). Classes 1 and 3 consisted of both auxiliary cells and ATGs, and had significantly different levels of all the metabolites tested. Further, AOIs on auxiliary cells and ATGs from tissue containing taurine-labeled ORNs fell into Class 1 (Fig. 7A, blue AOIs, Fig. 7F, G), while AOIs on auxiliary cells

and ATGs from tissue without taurine-labeled ORNs fell predominantly into Class 3 (Fig. S5; See Discussion). High levels of taurine separated Class 4 ORNs (Fig. 5A, green AOIs, Fig. 5F, G, I, arrow) from Classes 1-3. Class 5 consisted of the connective tissue between ORN clusters (Fig. 5A, cyan AOIs, Fig. 5C, arrowhead) and was distinguished from Class 6 ORNs (Fig. 5A, magenta AOIs, Fig. 5F, G, I, arrow) by lower arginine, glutamate, and glycine content. The lobster antennule had the fewest classes of all the species examined, and was distinguished from the vertebrates by its high arginine and reduced taurine labeling in most ORNs.

Immunohistochemistry of squid OE

In the squid, the pseudostratified olfactory epithelium contains at least five different morphological types of ORNs (types 1-5), and at least one support-like cell type (Emery, 1975). Three of the ORN subtypes (types 3, 4 and 5) have large invaginated cilia pockets. Cilia pockets retain access to the external environment and the cilia within them contain signal transduction proteins (Lucero et al., 2000;Mobley et al., 2007). Arginine labeled the type 2 cells, which have a small cell body in the middle layer of the OE, and a long dendrite ending in a knob-like structure at the apical surface (Fig. 9A, arrow). Aspartate labeled a subset of the type 2 cells (Fig. 9B, arrow), with lower labeling in the cilia pockets of cell types 3, 4 and 5 (Fig. 9B, asterisk). Glutamate labeling of the squid OE was found in three subsets of arginine-positive type 2 cells (Fig. 9C), but did not label the cilia pockets. Glycine outlined the type 3 cells, which have a cilia pocket in the apical layer of the OE (Fig. 9D, black arrowhead). The type 3 cilia pocket is connected to its cell body, located in the mid to basal layer of the OE, by a narrow isthmus. We observed glutathione labeling in types 2, 3 and 4 ORNs, but not in cilia pockets (Fig. 9E). Taurine labeling was high in the OE and did not distinguish any cell types, except to be either absent or at low levels in cilia pockets (Fig. 9F). In terms of overall intensity, arginine, aspartate and taurine had higher labeling than glutamate, glycine and glutathione. Based on the

images analyzed, we found that arginine labeling is high in type 2 ORNs with medium labeling in type 5 ORN somas and support cells. Aspartate labels type 2 ORNs and support cells, glutamate labels type 2 and 4 ORNs, glycine labels type 3 ORNs, glutathione labels type 2, 3 and 4 ORNs, and taurine labels most cells but is low in the cilia pockets. The type 1 ORNs are rare and difficult to identify; they are distinguished by an absence of glutamate and glutathione (Fig. 9C, arrow).

Squid OE cell types have multiple labeling patterns

In the squid OE we found 12 distinct classes. Classes 1, 4-6, 8, 10 and 12 consisted of AOIs from all three animals. Class 11 came from two different animals. Classes 3 and 7 represent single cells that came from one of two different animals. Classes 2 and 9 represent rare cells found in a single animal. The first branch of the dendrogram separated Classes 8-12, which had lower labeling levels, particularly for arginine and aspartate, from Classes 1-7 of the squid OE (Fig. 10). Considering Classes 1-7 first, the Class 7 type 2 ORN was distinguished from Classes 1-6 by glutamate labeling (Fig. S6, purple AOI). Class 5 (Fig. 9A, cyan AOIs, Fig. 9C, G, I, arrowhead) and 6 (Fig. 9A, magenta AOIs, Fig. 9E, G, arrowhead) type 2 ORNs were distinguished from Classes 1-4 based on their higher glutamate and glutathione, and from each other based on arginine labeling. Class 4 type 2 ORNshad higher levels of arginine (Fig. 9A, green AOIs) than Classes 1-3. Class 3 appeared to be a type 1 cell based on morphology and had a low glutamate profile (Fig. 9A, red AOI, Fig. C, G, arrow). Class 1 type 2 ORNs (Fig. 9A, blue AOIs, Fig. 9H) and Class 2 support cells could be distinguished by glutathione levels (Fig. S6, yellow AOIs). The cluster analysis did not distinguishtype 3, 4 and 5 somas as unique classes. Classes 8-12 identified type 3, 4 and 5 cilia pockets. Class 8 consisted mainly of type 3 and 4 cilia pockets (Fig. 9A, peach AOIs, Fig. 9B, H, arrowhead), which were distinguished by low aspartate, glutamate and glutathione labeling. Class 9 AOIs were found on type 3 and 5 cilia

pockets (Fig. S6, orange AOIs), which were distinguished from Classes 10-12 by high glutathione content. Other type 3 and 4 cilia pockets comprised Class 10 (Fig. 9A, cream AOIs, Fig. 9D, H, arrowhead) and were separated from classes 11-12 by glutathione and glycine labeling. Both Classes 11 and 12 contained the type 3 cilia pockets, however, Class 11 (Fig. 9A, pink AOIs, Fig. 9F, arrowhead) had lower levels of glutamate, glutathione and taurine than Class 12 (Fig. 9A maroon AOI, Fig. 9E, G, arrow). From the cluster analysis, we showed that across animals, squid ORN subtypes had different but overlapping metabolite profiles. Collectively, the six metabolites we tested identified four classes of cilia pocket labeling, seven classes of ORNs, and one support cell class.

Comparison of metabolite profiles across all species

To determine if metabolite profiles for analogous cell types are conserved across species, we used hierarchical cluster analysis to classify the mean metabolite values for each cell class from each tissue. Six statistically significant classes were identified (MANOVA, post-hoc test; $p < 0.05$). The dendrogram showed that the initial branch separated Class 6 from Classes 1-5 based on high aspartate levels. Class 6 contained one rare VN class from the mouse VNO and four lobster classes: three ORN classes and one outer auxiliary class. The next branch separated Classes 1-2 from Classes 3-5 based on their significantly lower glutamate and glycine levels (Fig. 11A). Class 1 was distinguished from Class 2 by its higher glutamate and glutathione levels (Fig. 11B). Class 1 consisted of mouse and squid ORNs, mouse and lobster non-sensory classes, and mouse VNO connective tissue and ECs. Class 2 had the lowest glutamate, glycine, glutathione and taurine intensity of all the classes. Class 2 contained lobster secretory rosettes, squid type 3 cilia pockets and three different classes of non-sensory tissue: two from mouse VNO and one from mouse OE. On the other main branch of the dendrogram, Class 3 was separated from Class 4 based on significantly higher aspartate and lower glycine levels and had

the highest glutathione labeling compared to the other classes. Class 3 contained five of the six VN classes from the mouse, four non-sensory classes from the mouse, including the SCs of the VNO, and a respiratory epithelium class from the zebrafish. Class 4 had the lowest average arginine content of all the classes and contained four non-sensory zebrafish classes, the two zebrafish ORN classes and the mouse respiratory epithelium class. Class 5 consisted only of non-sensory cells from the zebrafish OE, which had the highest glycine and glutathione content comparatively.

From these data, we observe that within a species, statistical classification identifies many different cell types as unique classes based on their metabolite profiles. Across species, statistical classification does not group analogous cell types together because of metabolite differences. Indeed, neuronal tissue in one species does not necessarily have the same metabolite profile as neuronal tissue in all the other species. These data suggest that across species, analogous cell types have different metabolic requirements to accomplish a common function. We discuss these differences and their implications below.

Discussion

We used the technique of metabolite profiling to address the following three questions: 1) are metabolite profiles for functionally distinct cell types consistent across animals within a species? 2) are metabolite profiles for analogous cell types conserved across species? 3) will a comparative study of metabolite profiles in three model organisms inform us about metabolite roles in the less-studied squid olfactory organ? We found thatwithin a species, metabolite profiles for particular cell classes were generally consistent across the three animals examined, particularly in the cell types that made up the majority of the epithelium eg. ORNs or VNs, and SCs. Within species, we found several metabolite-based cell classifications thatmirror ed classifications based on function and/or receptor class expression. For example, the ensheathing

cells of both mouse OE and VNO classified together, demonstrating consistency of a known cell type across different tissues in the same species. In contrast, mouse ORNs and VNs did not classify together (see Figure 11) and express different receptor classes and G proteins (Berghard et al., 1996;Matsunami and Buck, 1997). In the VNO, the apical and basal VNs had different metabolite profiles, possibly reflecting the distinct metabolic demands of activating the different receptors and G proteins expressed by these two cell groups (Halpern et al., 1995; Herrada and Dulac, 1997; Ishii et al., 2003).

Across species, we found that while profiles of all six metabolites were not conserved among analogous cell types, specific metabolites were associated with certain cell types. For example, taurine was found at high levels in all ORNs except lobster. Glutathione levels were significantly higher in the SCs of mouse OE, VNO, the Class 5 NSE of zebrafish and the auxiliary cells of lobster, compared to the respective neurons (student's t-tests, $p < 0.05$; data not shown), suggesting that metabolic roles are conserved. To determine if a comparative study of metabolite profiles in the three model organisms inform us about metabolite roles in the less-studied squid olfactory organ we review the physiological role of the six metabolites examined, our findings for each organism, and then compare our findings to the squid.

Metabolites

Arginine is a substrate for the nitric oxide synthase (NOS) pathway where the enzyme NOS converts arginine to nitric oxide gas (Mayer et al., 1991), which then acts as a diffusible second messenger and activates soluble guanylyl cyclases. The K_m of NOS for L-arginine is 16.5 µM, which is below the detection level of our immunocytochemical assay (100 µM) (Marc et al., 1990). Arginine is also important for cells either undergoing proliferation (Rodriguez et al., 2007) or stress as in tumors and wound healing (Tong and Barbul, 2004;Wheatley, 2005).

Aspartate is important for conversion to glutamate (Simon et al., 1967). In some species there is evidence for a role in neurotransmission (Shank et al., 1975;Constanti and Nistri, 1978;D'Aniello et al., 2005).

Glutamate is an important byproduct of the citric acid cycle, and is involved in numerous metabolic pathways. Besides its incorporation into proteins and peptides such as glutathione (Bukowska, 2004), glutamate is also an important neurotransmitter (Takeuchi, 1987;Sassoe-Pognetto et al., 1993;Berkowicz et al., 1994;Ennis et al., 1996)

Glycine is a neurotransmitter that gates anion channels (Betz, 1992) leading to membrane hyperpolarization, thus inhibiting the cell from depolarizing (Legendre, 2001). Metabolically, glycine is a byproduct of the citric acid cycle that can be used to make porphyrins, which lead to pathways for the production of hemoglobin and cytochromes (Beri and Chandra, 1993).

Glutathione is an important antioxidant, which can reduce oxidative damage to lipids, proteins and nucleic acids from oxygen radicals and hydrogen peroxide that are continually produced as byproducts of aerobic metabolism (Halliwell and Gutteridge, 1989;Stadtman, 1992). Glutathione can be conjugated by the enzyme glutathione S-transferase to a large number of electrophilic alkylating compounds, in order to protect cells from potential toxicity (Mannervik and Danielson, 1988;Pickett and Lu, 1989).

A neurochemical role for taurine was identified in coelenterates (Anderson and Spencer, 1989;Carlberg et al., 1995), and it is an important osmolyte for intracellular osmoregulation in mammals (Lambert, 2004). Studies have shown that taurine is abundant in the brains of both invertebrates (Evans, 1973;Schäfer et al., 1988) and vertebrates (Sturman, 1993).

Specific roles found for metabolites that are unique to a species are described below and we assume that the metabolites are also utilized for the functions described above.

Mouse Olfactory Epithelium

In the mouse OE, unique metabolite profiles identified many of the cell types that have been reported previously. Mouse ORNs had very low levels of all metabolites tested except for taurine. Hierarchical analysis did not differentiate the immature receptor neurons from mature ORNs, nor did it uniquely classify the two types of basal progenitor cells (horizontal and globose). A relatively rare class having high aspartate and glutamate was found in the apical OE and may correspond to microvillar cells (Elsaesser et al., 2005) (Fig. 1A, orange AOIs, Fig. 1C, G, I, arrowhead). Arginine was an excellent marker for the ECs, which have been shown to promote neurite extension (Kafitz and Greer, 1999) during development.

Consistent with the presence of glutathione peroxidase, reductase and S-transferase in rodent sustentacular cells and Bowman's glands, the high glutathione levels suggest a protective role against oxidative stress and xenobiotic-derived oxidants (Genter et al., 1995;Reed et al., 2003).

Mouse Vomeronasal Organ

In the mouse VNO, the SCs, VNs, connective tissue, ensheathing cells, glands and blood vessels each displayed unique metabolite profiles. Six classes of VNs were distinguished by heterogeneous labeling among the apical and basal VN populations. VN heterogeneity between the apical and basal layers is also reflected in patterns of receptor gene and G-protein expression (Halpern et al., 1995;Herrada and Dulac, 1997;Ishii et al., 2003). The apical VNs express the V1r genes and the G-protein subunit $G\alpha_{i2}$. The basal VNs express the V2r genes, the G-protein subunit $G\alpha_o$ and the class 1 genes of the major histocompatibility complex gene family H2-Mv (Ishii et al., 2003). Glycine's presence at high levels in basal VNs may indicate an inhibitory function.

Zebrafish Olfactory Epithelium

Our study identified many of the cell types described by Hansen and Zeiske (1998) in adult zebrafish OE; however, crypt cells were not identified as a unique cell class by our metabolite panel. The two ORN classes most likely represent the ciliated (basal) and microvillar (apical) cells (Lipschitz and Michel, 2002) (Fig. 5C, G, I). Hierarchical analysis clearly identified putative glycine-rich basal cells (Fig. 5D, arrow). Classes 3 and 5 most likely represent the goblet and ciliated non-sensory cells, respectively (Fig. 5B, E, G, H). As in the mouse VNO, we found unique metabolite profiles for neuronal cell types that have different morphologies, locations in the OE, and receptor expression (Sato et al., 2005). Indeed, basal ciliated ORNs express the OR type odorant receptors, cyclic nucleotide-gated channels, and had high glutamate labeling. Apical microvillar ORNs express the V2R-type receptors, transient receptor potential C2 channels (Hansen and Zielinski, 2005), and had higher aspartate, glutamate and glutathione labeling than the basal ORNs

Comparatively, zebrafish and mouse OE were similar in that both had very little arginine labeling, and higher glutathione labeling in the NSE than OE. The main difference in zebrafish from the other species was high glycine labeling in both sensory and non-sensory tissue. Interestingly, glycine and glutamate are the third and fourth most common amino acids in seven different tissues of another freshwater fish, *Rasbora daniconius* (Raizada et al., 1979). While a role for free glycine has not yet been shown in the olfactory system of freshwater fish, one study found that the presence of glycine increased tolerance to lethal concentrations of lead and mercury (Coello and Khan, 1996). It is not know if glycine is playing a protective role or contributing to pH regulation, as suggested by Raizada et al. (1979).

Lobster Olfactory Antennules

In the lobster, we identified three classes of ORNs, and four types of non-sensory tissue. Compared to the vertebrate species we examined, lobster olfactory tissue differed in four of the

six metabolites: the majority of lobster sensory ORNs lacked taurine, but had high arginine labeling. High glycine and aspartate labeling was confined to the ORNs.

The three lobster ORN classes are based on differences in taurine levels. A study by Steullet et al. (2000) showed that ORNs in the proliferative zone, located at the proximal end of the aesthetasc region, had high levels of taurine, while mature ORNs lacked taurine labeling. Thus, the two classes of auxiliary cells and ATGs (Classes 1 and 3) as well as the three classes of ORNs we observed may reflect maturational states. While there is evidence for a neuroprotective role in human fetal brain neurons (Chen et al., 1998), taurine's role in the development of lobster ORNs is unknown.

Compared to the vertebrates, lobster ORNs had high levels of aspartate and glycine. The amino acids utilized for osmoregulation may vary between cell types and species (Gilles, 1978;Pierce and Amende, 1981), but is always some combination of non-essential amino acids such as glycine, alanine, proline, glutamate, taurine and sometimes aspartate and glutamine (Pierce, 1982). Mature lobsterORNs may be using a spartate and glycine instead of taurine for osmoregulation (Fig. 7B, D). Aspartate may also be enhancing glutamatergic neurotransmission (Shank and Freeman, 1975;Constanti and Nistri, 1978;Constanti and Nistri, 1979). In the lobster neuromuscular junction, aspartate and glutamate cooperatively increase activation of glutamate receptors. While L-glutamate receptors have been described in the lobster olfactory organ (Burgess and Derby, 1997), their ability to bind aspartate has not been examined.

Medium glutathione levels in lobster outer auxiliary cells were significantly lower than that in mouse VNO SCs. Currently, it is not known whether xenobiotic metabolism occurs in the olfactory antennules of lobster. In the digestive gland of the American lobster *Homarus americanus,* glutathione plays a detoxifying role by making a transient complex with copper-metallothioneins and is then released as a copper-glutathione complex (Brouwer and Brouwer-

Hoexum, 1991). It is possible that a copper-glutathione complex is also present in lobster olfactory tissue.

The majority of lobster ORNs had high arginine levels. It is unlikely that the majority of lobster ORNs are undergoing proliferation (Tong and Barbul, 2004;Wheatley, 2005;Rodriguez et al., 2007), The few ORNs that are high in taurine (a marker of proliferating cells in lobster) are low in arginine (Fig. 7A, F, yellow, green and magenta AOIs). Studies on other lobster species have shown that the arginine requirements for protein metabolism are higher than in other crustaceans (Mente et al., 2001) and that lobster proteins also have more arginine content than other crustaceans (Camien et al., 1951;Mason and Castell, 1980). Finally, the high arginine may contribute to nitric oxide signaling however, NOS has not been identified in lobster olfactory antennules.

Squid Olfactory Epithelium

Metabolite profiling of squid OE identified both the morphologically distinct cell types (types 1-5) as well as differences between cilia pockets. A priori, we expected each morphological subtype to have a unique metabolite profile. Instead, we found that within the morphologically defined cell types there are several metabolite profiles. The type 2, 3, 4 and 5 ORNseach segregated into more than one class of ce lls. This is consistent with a previous study that demonstrated expression of multiple combinations of signaling proteins in single squid ORNs(Mobley et al., 2007) . For example, the type 3, 4 and 5 neurons express both $G\alpha_q$ and $G\alpha_{olf}$ with differential co-localization to the cilia pockets. Our findings in squid are consistent with results from mouse VNO and zebrafish; morphology, expression of different proteins and/or receptor classes are reflected in heterogeneous metabolite labeling.

Arginine labeling was high in subsets of type 2 and 5 ORNs. The location of arginine-labeled cells within the squid OEuled out the possibility that they were ensheathing cells as in

mouse OE and VNO. The differentiated morphology of type 2 and 5 ORNs reduce the likelihood that they are proliferative. A role for arginine in nitric oxide signaling is supported by studies showing that antibodies against neuronal NOS labeled cells in the squid OE (Lucero and Sitthichai, 2003) and the olfactory lobe of the cephalopod *Sepia officinalis* (Di Cosmo et al., 2000). Cephalopods may be more similar to lobsters in that they require or have higher levels of arginine in general.

L-Glutamate and L-aspartate are the second and sixth most abundant free amino acid, respectively in the optic lobe and stellate ganglion of the squid *L. vulgaris* (D'Aniello et al., 1995). Glutamate is a neurotransmitter in several neuronal systems of the squid (Eusebi et al., 1985;Florey et al., 1985;de Santis and Messenger, 1989;Lieberman and Sanzenbacher, 1992;Evans et al., 1992a;Evans et al., 1992b;Tu and Budelmann, 1994;Di Cosmo et al., 1999;Loi and Tublitz, 2000;Lima et al., 2003). Evidence in the retina of *S. officinalis* suggests a modulatory role for L-aspartate in a cephalopod sensory system (D'Aniello et al., 2005). L-glutamate and both D- and L-aspartate were shown to gate an AMPA-like glutamate receptor that was isolated from the stellate ganglion/giant fiber lobe complex of *Loligo opalescens* (Battaglia et al., 2003) and expressed in HEK293 cells (Brown et al., 2006). Glutamate was only observed in a subset of type 2 squid ORNs (Classes 4, 5 and 7), while aspartate labeling was only found in Class 4 of type 2 squid ORNs and was absent in type 3 and 4 ORNs, suggesting a specific role for these metabolites in a subset of ORNs. Glutamate may be used as a neurotransmitter in a subset of squid ORNs.

It is not known what role glycine and glutathione have in the cephalopod olfactory system. Glycine acts at several synapses of the squid central nervous system (Caldwell and Lea, 1978;Horn, 1986;Vinogradova et al., 2002;Lima et al., 2003), but since there is no clear role for glycine in our model organisms we cannot draw any conclusions about the role of glycine in

squid. There were two classes of cells in squid OE that had high glutathione labeling (Classes 5 and 6), and were morphologically identified as a subset of type 2 cells. The identified Class 1 SCs had medium glutathione levels, however, based on glutathione in our model systems, the squid Class 5 and 6 cells may actually be a second type of support cell.

Taurine is the most abundant free amino acid in the ink of one octopus and three squid species (Derby et al., 2007) and is also found in the optic lobes and stellate ganglion of *L. vulgaris* (D'Aniello, et al., 1995). Our data showed that taurine levels in the squid OE had the highest average pixel intensity compared to the other metabolites we tested. Marine mollusks commonly have high concentrations of taurine, and it may play an important role in the osmoregulation of the ORNs as they are directly exposed to the aquatic environment.

Collectively, these data describe a diverse population of ORNs in the squid olfactory organ. Although the ORNs share a common function, to transduce odors, some contain high levels of different metabolites that are present for additional functions.

Comparison of sensory tissues across species

In a comparison of chemosensory tissues across species, we found interesting similarities, differences and patterns. We were able to make some predictions about the function of cells in the squid OE based on what we know about metabolite roles in our three model organisms, mouse, zebrafish and lobster. Due to significant differences in at least one metabolite, analogous cell types across species were not grouped within the same class. For example, the high arginine and low taurine content in lobster statistically separated its ORN classes from those of other species. High glycine content throughout the zebrafish OE separated most of its cell classes from the other species.

Strong similarities have been found in comparing retinal metabolite profiles across species such as primate (Kalloniatis et al., 1996), cat (Marc et al., 1998) rabbit (Marc and Jones,

2002), zebrafish (Marc and Cameron, 2001), and goldfish (Marc et al., 1995). There are several factors that we hypothesize are contributing to the differences in olfactory system metabolite profiles. The first is due to direct contact with different environments that put different osmotic constraints on the animals. Secondly, the level of oxygen exposure may influence the levels of antioxidants, such as glutathione, in the epithelia. Thirdly, the different types of toxins that are metabolized or protected against may influence the metabolites present in the epithelia. When protective mechanisms are overwhelmed, toxins can result in cell death and in four of the five tissues we examined (mouse OE, VNO, zebrafish and lobster), regeneration of neurons has been demonstrated (Harrison et al., 2001;Schwob, 2002;Martinez-Marcos et al., 2005;Zupanc et al., 2005). Neurons of different ages may have different metabolic requirements, contributing to changing metabolite profiles. Although chemosensory systems across species share many similarities, the heterogeneous environments, osmotic and toxicant exposure create differences that are reflected in their metabolite profiles.

Acknowledgements

Thanks to Dr. C. Derby for providing the lobster tissue, Dr. M. Eram, Dr. B. Jones, K. Davis, F. Solelbi, P. Deng, and D. Elkin for technical support. This work was supported by a grant from the National Institute of Health NRSA 1 F31 DC006793-01 to A.S.M. and PO1 NS017938 to M.T.L. and W.C.M.

UU IR Author Manuscript

Reference List

Ache BW (1994) Towards a common strategy for transducing olfactory information. Seminars in Cell Biology 5: 55-63.

Ache BW, Derby CD (1985) Functional organization of olfaction in crustaceans. TINS 8: 356-360.

Anderson PAV, Spencer AN (1989) The importance of cnidarian synapses for neurobiology. J Neurobiol 20: 435-457.

Battaglia AA, Nardi G, Steinhardt A, Novakovic A, Gentile S, Iaccarino IP, Gilly WF, de Santis A (2003) Cloning and characterization of an ionotropic glutamate receptor subunit expressed in the squid nervous system. Eur J Neurosci 17: 2256-2266.

Beauchamp GK, Yamazaki K (2003) Chemical signalling in mice. Biochem Soc Trans 31: 147-151.

Berghard A, Buck LB, Liman ER (1996) Evidence for distinct signaling mechanisms in two mammalian olfactory sense organs. Proc Natl Acad Sci U S A 93: 2365-2369.

Beri R, Chandra R (1993) Chemistry and biology of heme. Effect of metal salts, organometals, and metalloporphyrins on heme synthesis and catabolism, with special reference to clinical implications and interactions with cytochrome P-450. Drug Metab Rev 25: 49-152.

Berkowicz DA, Trombley PQ, Shepherd GM (1994) Evidence for glutamate as the olfactory receptor cell neurotransmitter. J Neurophysiol 71: 2557-2561.

Betz H (1992) Structure and function of inhibitory glycine receptors. Q Rev Biophys 25: 381-394.

Bringmann A, Pannicke T, Grosche J, Francke M, Wiedemann P, Skatchkov SN, Osborne NN, Reichenbach A (2006) Müller cells in the healthy and diseased retina. Prog Retin Eye Res 25: 397-424.

Brouwer M, Brouwer-Hoexum T (1991) Interaction of copper-metallothionein from the American lobster, *Homarus americanus*, with glutathione. Arch Biochem Biophys 290: 207-213.

Brown ER, Piscopo S, Chun JT, Francone M, Mirabile I, D'Aniello A (2006) Modulation of an AMPA-like glutamate receptor (SqGluR) gating by L- and D-aspartic acids. Amino Acids 32: 53-57.

Bukowska B (2004) [Glutathione: its biosynthesis, induction agents and concentrations in selected diseases.]. Med Pr 55: 501-509.

Burgess MF, Derby CD (1997) Two novel types of L-glutamate receptors with affinities for NMDA and L-cysteine in the olfactory organ of the Caribbean spiny lobster *Panulirus argus*. Brain Res 771: 292-304.

Caldwell PC, Lea TJ (1978) Glycine fluxes in squid giant axons. J Physiol 278: 1-25.

Camien MN, Sarlet H, Cuchateau F, Florkin M (1951) Nonprotein amino acidss in muscle and blood of marine and fresh water Crustacea. J Biol Chem 193: 881-885.

Carlberg M, Alfredsson K, Nielsen SO, Anderson PAV (1995) Taurine-like immunoreactivity in the motor nerve net of the jellyfish *Cyanea capillata*. Biol Bull 188: 78-82.

Chen XC, Pan ZL, Liu DS, Han X (1998) Effect of taurine on human fetal neuron cells: proliferation and differentiation. Adv Exp Med Biol 442: 397-403.

Coello WF, Khan MA (1996) Protection against heavy metal toxicity by mucus and scales in fish. Arch Environ Contam Toxicol 30: 319-326.

Constanti A, Nistri A (1978) A study of the interactions between glutamate and aspartate at the lobster neuromuscular junction. Br J Pharmacol 62: 495-505.

Constanti A, Nistri A (1979) Further observations on the interaction between glutamate and aspartate on lobster muscle. Br J Pharmacol 65: 287-301.

D'Aniello A, Nardi G, de Santis A, Vetere A, Di Cosmo A, Marchelli R, Dossena a, Fisher G (1995) Free L-amino acids and D -aspartate content in the nervous system of Cephalopoda. A comparative study. Comp Biochem Physiol 112B: 661-666.

D'Aniello S, Spinelli P, Ferrandino G, Peterson K, Tsesarskia M, Fisher G, D'Aniello A (2005) Cephalopod vision involves dicarboxylic amino acids: D-aspartate, L-aspartate and L-glutamate. Biochem J 386: 331-340.

de Santis A, Messenger JB (1989) New evidence that L-glutamate is a transmitter at the squid giant synapse. Q J Exp Physiol 74: 219-222.

Derby CD, Kicklighter CE, Johnson PM, Zhang X (2007) Chemical Composition of Inks of Diverse Marine Molluscs Suggests Convergent Chemical Defenses. J Chem Ecol.

Di Cosmo A, Di Cristo C, Palumbo A, d'Ischia M, Messenger JB (2000) Nitric oxide synthase (NOS) in the brain of the cephalopod *Sepia officinalis*. J Comp Neurol 428: 411-427.

Di Cosmo A, Nardi G, Di Cristo C, de Santis A, Messenger JB (1999) Localization of L-glutamate and glutamate-like receptors at the squid giant synapse. Brain Res 839: 213-220.

Di Giorgi Gerevini V, Caruso A, Cappuccio I, Ricci VL, Romeo S, Della RC, Gradini R, Melchiorri D, Nicoletti F (2004) The mGlu5 metabotropic glutamate receptor is expressed in zones of active neurogenesis of the embryonic and postnatal brain. Brain Res Dev Brain Res 150: 17-22.

Ebbesson SO, Smith J, Co C, Ebbesson LO (1996) Transient alterations in neurotransmitter levels during a critical period of neural development in coho salmon (*Oncorhyncus kisutch*). Brain Res 742: 339-342.

Eisthen HL (2002) Why are olfactory systems of different animals so similar? Brain Behav Evol 59: 273-293.

Elsaesser R, Montani G, Tirindelli R, Paysan J (2005) Phosphatidyl-inositide signalling proteins in a novel class of sensory cells in the mammalian olfactory epithelium. European Journal of Neuroscience 21: 2692-2700.

Emery DG (1975) The histology and fine structure of the olfactory organ of the squid *Lolliguncula brevis* Blainville. Tissue & Cell 7: 357-367.

Ennis M, Zimmer LA, Shipley MT (1996) Olfactory nerve stimulation activates rat mitral cells via NMDA and non-NMDA receptors in vitro. Neuroreport 7: 989-992.

Eram M, Michel WC (2005) Morphological and biochemical heterogeneity in facial and vagal nerve innervated taste buds of the channel catfish, *Ictalurus punctatus*. J Comp Neurol 486: 132-144.

Eusebi F, Miledi R, Parker I, Stinnakre J (1985) Post-synaptic calcium influx at the giant synapse of the squid during activation by glutamate. J Physiol 369: 183-197.

Evans PD (1973) Amino acid distribution in the nervous system of the crab, *Carcinus maenas* (L.). J Neurochem 21: 11-17.

Evans PD, Reale V, Merzon RM, Villegas J (1992a) N-methyl-D-aspartate (NMDA) and non-NMDA (metabotropic) type glutamate receptors modulate the membrane potential of the Schwann cell of the squid giant nerve fibre. J Exp Biol 173: 229-249.

Evans PD, Reale V, Merzon RM, Villegas J (1992b) The effect of a glutamate uptake inhibitor on axon-Schwann cell signalling in the squid giant nerve fibre. J Exp Biol 173: 251-260.

Florey E, Dubas F, Hanlon RT (1985) Evidence for L-glutamate as a transmitter substance of motoneurons innervating squid chromatophore muscles. Comp Biochem Physiol C 82: 259-268.

Gasic GP, Heinemann S (1991) Receptors coupled to ionic channels: the glutamate receptor family. Curr Opin Neurobiol 1: 20-26.

Genter MB, Owens DM, Deamer NJ (1995) Distribution of microsomal epoxide hydrolase and glutathione S-transferase in the rat olfactory mucosa: relevance to distribution of lesions caused by systemically-administered olfactory toxicants. Chem Senses 20: 385-392.

Gilles R (1978) Intracellular free amino acids and cell volume regulation during osmotic stresses. In: Osmotic and Volume Regulation (Jergensen CB, Skadhauge E, eds), pp 470-491.

Grünert U, Ache BW (1988) Ultrastructure of the aesthetasc (olfactory) sensilla of the spiny lobster, *Panulirus argus*. Cell Tissue Res 251: 95-103.

Halliwell B, Gutteridge JMC (1989) Free Radicals in Biology and Medicine. Oxford: Clarendon Press.

Halpern M, Shapiro LS, Jia C (1995) Differential localization of G proteins in the opossum vomeronasal system. Brain Res 677: 157-161.

Hansen A, Zeiske E (1998) The peripheral olfactory organ of the zebrafish, *Danio rerio*: an ultrastructural study. Chemical Senses 23: 39-48.

Hansen A, Zielinski BS (2005) Diversity in the olfactory epithelium of bony fishes: development, lamellar arrangement, sensory neuron cell types and transduction components. J Neurocytol 34: 183-208.

Harrison PJ, Cate HS, Swanson ES, Derby CD (2001) Postembryonic proliferation in the spiny lobster antennular epithelium: rate of genesis of olfactory receptor neurons is dependent on molt stage. J Neurobiol 47: 51-66.

Hayes JD, McLellan LI (1999) Glutathione and glutathione-dependent enzymes represent a co-ordinately regulated defence against oxidative stress. Free Radic Res 31: 273-300.

Herrada G, Dulac C (1997) A novel family of putative pheromone receptors in mammals with a topographically organized and sexually dimorphic distribution. Cell 90: 763-773.

Hertz L, Peng L (1992) Energy metabolism at the cellular level of the CNS. Can J Physiol Pharmacol 70 Suppl: S145-S157.

Horn LW (1986) Measurements of amino acid transport in internally dialyzed giant axons. J Membr Biol 89: 185-192.

Ishii T, Hirota J, Mombaerts P (2003) Combinatorial coexpression of neural and immune multigene families in mouse vomeronasal sensory neurons. Curr Biol 13: 394-400.

Jia C, Halpern M (1996) Subclasses of vomeronasal receptor neurons: differential expression of G proteins (Gi alpha 2 and G(o alpha)) and segregated projections to the accessory olfactory bulb. Brain Res 719: 117-128.

Jones BW, Watt CB, Frederick JM, Baehr W, Chen CK, Levine EM, Milam AH, Lavail MM, Marc RE (2003) Retinal remodeling triggered by photoreceptor degenerations. J Comp Neurol 464: 1-16.

Kafitz KW, Greer CA (1999) Olfactory ensheathing cells promote neurite extension from embryonic olfactory receptor cells in vitro. Glia 25: 99-110.

Kalloniatis M, Marc RE, Murry RF (1996) Amino acid signatures in the primate retina. J Neurosci 16: 6807-6829.

Koehl MA, Koseff JR, Crimaldi JP, McCay MG, Cooper T, Wiley MB, Moore PA (2001) Lobster sniffing: antennule design and hydrodynamic filtering of information in an odor plume. Science 294: 1948-1951.

Korsching SI, Argo S, Campenhausen H, Friedrich RW, Rummrich A, Weth F (1997) Olfaction in zebrafish: what does a tiny teleost tell us? Semin Cell Dev Biol 8: 181-187.

Lambert IH (2004) Regulation of the cellular content of the organic osmolyte taurine in mammalian cells. Neurochem Res 29: 27-63.

Laverack MS (1964) The antennular sense organs of *Panulirus argus*. Comp Biochem Physiol 13: 301-321.

Legendre P (2001) The glycinergic inhibitory synapse. Cell Mol Life Sci 58: 760-793.

Lieberman EM, Sanzenbacher E (1992) Mechanisms of glutamate activation of axon-to-Schwann cell signaling in the squid. Neuroscience 47: 931-939.

Lima PA, Nardi G, Brown ER (2003) AMPA/kainate and NMDA-like glutamate receptors at the chromatophore neuromuscular junction of the squid: role in synaptic transmission and skin patterning. Eur J Neurosci 17: 507-516.

Lipschitz DL, Michel WC (2002) Amino acid odorants stimulate microvillar sensory neurons. Chem Senses 27: 277-286.

Loi PK, Tublitz NJ (2000) Roles of glutamate and FMRFamide-related peptides at the chromatophore neuromuscular junction in the cuttlefish, *Sepia officinalis*. J Comp Neurol 420: 499-511.

Lucero MT, Huang W, Dang T (2000) Immunohistochemical evidence for the Na+/Ca2+ exchanger in squid olfactory neurons. Philosophical Transactions of the Royal Society of London, B 355: 1215-1218.

Lucero MT, Sitthichai A (2003) Evidence for the nitric oxide pathway in squid olfactory receptor neurons. Jpn J Taste Smell Res 9: 277-278.

Mannervik B, Danielson UH (1988) Glutathione transferases--structure and catalytic activity. CRC Crit Rev Biochem 23: 283-337.

Marc RE, Cameron D (2001) A molecular phenotype atlas of the zebrafish retina. J Neurocytol 30: 593-654.

Marc RE, Jones BW (2002) Molecular phenotyping of retinal ganglion cells. J Neurosci 22: 413-427.

Marc RE, Liu WL, Kalloniatis M, Raiguel SF, Van Haesendonck E (1990) Patterns of glutamate immunoreactivity in the goldfish retina. J Neurosci 10: 4006-4034.

Marc RE, Murry RF, Basinger SF (1995) Pattern recognition of amino acid signatures in retinal neurons. J Neurosci 15: 5106-5129.

Marc RE, Murry RF, Fisher SK, Linberg KA, Lewis GP, Kalloniatis M (1998) Amino acid signatures in the normal cat retina. Invest Ophthalmol Vis Sci 39: 1685-1693.

Martinez Marcos A, Jia C, Quan W, Halpern M (2005) Neurogenesis, migration, and apoptosis in the vomeronasal epithelium of adult mice. J Neurobiol.

Mason EG, Castell JD (1980) The effects of supplementing purified proteins with limiting essential amino acids on growth and survival of juvenile lobsters, *Homarus americanus*. Proc World Maricult Soc 11: 346-354.

Matsunami H, Buck LB (1997) A multigene family encoding a diverse array of putative pheromone receptors in mammals. Cell 90: 775-784.

Mayer B, John M, Heinzel B, Werner ER, Wachter H, Schultz G, Bohme E (1991) Brain nitric oxide synthase is a biopterin- and flavin-containing multi-functional oxido-reductase. FEBS Lett 288: 187-191.

Menco BP, Carr VM, Ezeh PI, Liman ER, Yankova MP (2001) Ultrastructural localization of G-proteins and the channel protein TRP2 to microvilli of rat vomeronasal receptor cells. J Comp Neurol 438: 468-489.

Mendoza AS (1993) Morphological studies on the rodent main and accessory olfactory systems: the regio olfactoria and vomeronasal organ. Ann Anat 175: 425-446.

Mente E, Houlihan DF, Smith K (2001) Growth, feeding frequency, protein turnover, and amino acid metabolism in European lobster *Homarus gammarus* L. J Exp Zool 289: 419-432.

Michel WC, Steullet P, Cate HS, Burns CJ, Zhainazarov AB, Derby CD (1999) High-resolution functional labeling of vertebrate and invertebrate olfactory receptor neurons using agmatine, a channel-permeant cation. J Neurosci Methods 90: 143-156.

Miranda-Contreras L, Ramirez-Martens LM, Benitez-Diaz PR, Pena-Contreras ZC, Mendoza-Briceno RV, Palacios-Pru EL (2000) Levels of amino acid neurotransmitters during mouse olfactory bulb neurogenesis and in histotypic olfactory bulb cultures. Int J Dev Neurosci 18: 83-91.

Mobley AS, Gandham M, Lucero MT (2007) Evidence for multiple signaling pathways in single squid olfactory receptor neurons. J Comp Neurol 501: 231-242.

Orlando L (2001) Odor detection in zebrafish. Trends Neurosci 24: 257-258.

Palaiologos G, Hertz L, Schousboe A (1989) Role of aspartate aminotransferase and mitochondrial dicarboxylate transport for release of endogenously and exogenously supplied neurotransmitter in glutamatergic neurons. Neurochem Res 14: 359-366.

Pickett CB, Lu AY (1989) Glutathione S-transferases: gene structure, regulation, and biological function. Annu Rev Biochem 58: 743-764.

Pierce SK (1982) Invertebrate cell volume control mechanisms: a coordinated use of intracellular amino acids and inorganic ions as osmotic solute. Biol Bull 163: 405-419.

UU IR Author Manuscript

Pierce SK, Amende LM (1981) Control mechanisms of amino acid mediated cell volume regulation in salinity stressed molluscs. J Exp Zool 215: 247-257.

Potter DW, Finch L, Udinsky JR (1995) Glutathione content and turnover in rat nasal epithelia. Toxicol Appl Pharmacol 135: 185-191.

Raizada AK, Jain AK, Dahiya MS (1979) Free amino acids in various tissues of a fresh-water teleost, *Rasbora daniconius* (Ham). I. Qualitative analysis. Biochem Exp Biol 15: 53-55.

Reed CJ, Robinson DA, Lock EA (2003) Antioxidant status of the rat nasal cavity. Free Radic Biol Med 34: 607-615.

Rodriguez PC, Quiceno DG, Ochoa AC (2007) L-arginine availability regulates T-lymphocyte cell-cycle progression. Blood 109: 1568-1573.

Sassoe-Pognetto M, Cantino D, Panzanelli P, Verdun dC, Giustetto M, Margolis FL, De Biasi S, Fasolo A (1993) Presynaptic co-localization of carnosine and glutamate in olfactory neurones. Neuroreport 5: 7-10.

Sato Y, Miyasaka N, Yoshihara Y (2005) Mutually exclusive glomerular innervation by two distinct types of olfactory sensory neurons revealed in transgenic zebrafish. J Neurosci 25: 4889-4897.

Schäfer S, Bicker G, Ottersen OP, Storm-Mathisen J (1988) Taurine-like immunoreactivity in the brain of the honeybee. J Comp Neurol 268: 60-70.

Schmidt M, Chien H, Tadesse T, Johns ME, Derby CD (2006) Rosette-type tegumental glands associated with aesthetasc sensilla in the olfactory organ of the Caribbean spiny lobster, *Panulirus argus*. Cell Tissue Res 325: 369-395.

Schwob JE (2002) Neural regeneration and the peripheral olfactory system. Anat Rec 269: 33-49.

Shank RP, Freeman AR (1975) Cooperative interaction of glutamate and aspartate with receptors in the neuromuscular excitatory membrane in walking limbs of the lobster. J Neurobiol 6: 289-303.

Shank RP, Freeman AR, McBride WJ, Aprison MH (1975) Glutamate and aspartate as mediators of neuromuscular excitation in the lobster. Comp Biochem Physiol C 50: 127-131.

Simon G, Drori JB, Cohen MM (1967) Mechanism of conversion of aspartate into glutamate in cerebral-cortex slices. Biochem J 102: 153-162.

Stadtman ER (1992) Protein oxidation and aging. Science 257: 1220-1224.

Steinbusch HW, Verhofstad AA, Joosten HW (1978) Localization of serotonin in the central nervous system by immunohistochemistry: description of a specific and sensitive technique and some applications. Neuroscience 3: 811-819.

Steinbusch HW, Verhofstad AA, Joosten HW (1982) Antibodies to serotonin for neuroimmunocytochemical studies. J Histochem Cytochem 30: 756-759.

Steullet P, Cate HS, Derby CD (2000) A spatiotemporal wave of turnover and functional maturation of olfactory receptor neurons in the spiny lobster *Panulirus argus*. J Neurosci 20: 3282-3294.

Steullet P, Krutzfeldt DR, Hamidani G, Flavus T, Ngo V, Derby CD (2002) Dual antennular chemosensory pathways mediate odor-associative learning and odor discrimination in the Caribbean spiny lobster *Panulirus argus*. J Exp Biol 205: 851-867.

Sturman JA (1993) Taurine in development. Physiol Rev 73: 119-147.

Takeuchi A (1987) The transmitter role of glutamate in nervous systems. Jpn J Physiol 37: 559-572.

Tong BC, Barbul A (2004) Cellular and physiological effects of arginine. Mini Rev Med Chem 4: 823-832.

Torres GE, Amara SG (2007) Glutamate and monoamine transporters: new visions of form and function. Curr Opin Neurobiol.

Trinh K, Storm DR (2004) Detection of odorants through the main olfactory epithelium and vomeronasal organ of mice. Nutr Rev 62: S189-S192.

Trombley PQ, Shepherd GM (1993) Synaptic transmission and modulation in the olfactory bulb. Curr Opin Neurobiol 3: 540-547.

Tu Y, Budelmann BU (1994) The effect of L-glutamate on the afferent resting activity in the cephalopod statocyst. Brain Res 642: 47-58.

Vinogradova IM, Zajicek J, Gentile S, Brown ER (2002) Effect of glycine on synaptic transmission at the third order giant synapse of the squids *Alloteuthis subulata* and *Loligo vulgaris*. Neurosci Lett 325: 42-46.

Watanabe M, Shimada M, Watanabe H, Nakanishi M (1990) Amino acid content in several brain regions of the active and hibernating frog, *Rana esculenta*. Comp Biochem Physiol B 97: 605-610.

Wheatley DN (2005) Arginine deprivation and metabolomics: important aspects of intermediary metabolism in relation to the differential sensitivity of normal and tumour cells. Semin Cancer Biol 15: 247-253.

Zufall F, Kelliher KR, Leinders-Zufall T (2002) Pheromone detection by mammalian vomeronasal neurons. Microsc Res Tech 58: 251-260.

Zupanc GK, Hinsch K, Gage FH (2005) Proliferation, migration, neuronal differentiation, and long-term survival of new cells in the adult zebrafish brain. J Comp Neurol 488: 290-319.

Figure Legends

Figure 1. Mouse olfactory epithelium. **A:** Arginine (Arg). The image is marked to indicate the different layers of the olfactory epithelium (OE); arrowhead indicates the beginning of respiratory epithelium (RE). The AOI mask is overlaid and color coded by class (bottom): 1, blue; 2, yellow; 4, green; 5, cyan; 6, fuchsia; 7, purple; 9, orange (Classes 3 and 8 see Fig. S1). **B:** Aspartate (Asp). **C:** Glutamate (Glu). **D:** Glycine (Gly). **E:** GSH. **F:** Taurine (Tau). **G:** RGB image of Tau (red), Glu (green) and GSH (blue). **H:** RGB image of Arg (red), Asp (green), and Gly (blue). **I:**Higher magnification image of area within w hitedashed line in **G**. Numbers, arrows and arrowheads indicate the Class number. LP, lamina propria; SC, sustentacular cell; ORN, olfactory receptor neuron; OEC, olfactory ensheathing cell; CT, connective tissue; BV, blood vessel; dashed line in A indicates basal lamina. Scale bars = 10 µm.

Figure 2. Hierarchical classification of AOIs from mouse olfactory epithelium. **A:** Dendrogram of the hierarchical cluster analysis. Statistical significance of each class determined using MANOVA. Thick bars correspond to class divisions. **B:** Histogram of the mean values for each class.

Figure 3. Mouse vomeronasal epithelium. **A:** Arginine. The image is marked to indicate the different layers of the OE. The AOI mask is overlaid and color coded by class (right): 1, blue; 2, yellow; 4, green; 5, cyan; 6, fuchsia; 8, peach; 10, cream; 11, pink; 12, maroon (Classes 3, 7 and 9 see Fig. S2). **B:** Aspartate. **C:** Glutamate. **D:** Glycine. **E:** GSH. **F:** Taurine. **G-H:** RGB images of the mouse VNO. **I:**Higher magnification image of are a within white dashed line in **G**. Numbers, arrows and arrowheads indicate the Class number. aVN, apical vomeronasal

neurons; bVN, basal vomeronasal neurons; LP, lamina propria; basal lamina, dashed line in A. Scale bars = 10 µm.

Figure 4. Hierarchical classification of AOIs from mouse vomeronasal epithelium. **A:** Dendrogram of the hierarchical cluster analysis. Statistical significance of each class determined using MANOVA. Thick bars correspond to class divisions. **B:** Histogram of the mean values for each class.

Figure 5. Zebrafish olfactory epithelium. **A:** Arginine. The image is marked to indicate the main features of the OE; arrowhead indicates the beginning of non-sensory epithelium. The AOI mask is overlaid and color-coded (see legend in Fig. 3) by class: 1, blue; 2, yellow; 3, red; 4, green; 5, cyan; 7, purple (Classes 6 and 8 see Fig. S3). **B:** Aspartate. **C:** Glutamate. **D:** Glycine. **E:** GSH. **F:** Taurine. **G-H:** RGB images of the zebrafish OE. **I:**Higher magnification image of area within white dashed line in **G**. Numbers, arrows and arrowheads indicate the Class number. BL, basal lamina (dashed line in A). Scale bars: A = 10 µm, I = 5 µm.

Figure 6. Hierarchical classification of AOIs from zebrafish olfactory epithelium. **A:** Dendrogram of the hierarchical cluster analysis. Statistical significance of each class determined using MANOVA. Thick bars correspond to class divisions. **B**: Histogram of the mean values for each class.

Figure 7. Lobster olfactory (lateral) antennule. **A:** Arginine. The image is marked to indicate the main features of the antennule. The AOI mask is overlaid and color-coded (see legend in Fig. 3) by class: 1, blue; 2, yellow; 4, green; 5, cyan; 6, fuchsia; 7, purple (Class 3 see Fig. S4).

B: Aspartate. **C:** Glutamate. **D:** Glycine. **E:** GSH. **F:** Taurine. **G-H:** RGB images of the lobster olfactory antennule. **I:**Higher magnification image of area within w hite dashed line in **G**. Numbers, arrows and arrowheads indicate the Class number. ACs, auxiliary cells; ATG, aesthetasc tegumental gland; SR, secretory rosette. Scale bars = 10 µm.

Figure 8. Hierarchical classification of AOIs from the lobster olfactory antennule. **A:** Dendrogram of the hierarchical cluster analysis. Statistical significance of each class determined using MANOVA. Thick bars correspond to class divisions. **B**: Histogram of the mean values for each class.

Figure 9. Squid olfactory epithelium. **A:** Arginine. The image is marked to indicate the main features of the OE. The AOI mask is overlaid and color-coded (see legend in Fig. 3) by class: 1, blue; 3, red; 4, green; 5, cyan; 6, fuchsia; 8, peach; 10, cream; 11, pink; 12, maroon (Classes 2, 7 and 9 see Fig. S5). **B:** Aspartate. **C:** Glutamate. **D:** Glycine. **E:** GSH. **F:** Taurine. **G-H:** RGB images of the squid OE. **I:** Higher magnification image of area within white dashed line in **G**. Numbers, arrows and arrowheads indicate the Class number. CP, cilia pocket; CT, connective tissue; T2, type 2 ORN; T3, type 3 ORN; T4, type 4 ORN; T5, type 5 ORN; basal lamina; dashed line in A. Scale bars = 10 µm.

Figure 10. Hierarchical classification of AOIs from squid olfactory epithelium. **A:** Dendrogram of the hierarchical cluster analysis. Statistical significance of each class determined using MANOVA. Thick bars correspond to class divisions. **B**: Histogram of the mean values for each class.

Figure 11. Hierarchical cluster analysis of the means from all the animal classes. **A:** Dendrogram of the hierarchical cluster analysis. Thick bars correspond to class divisions. Class descriptions are listed opposite each branch of the dendrogram (Class number from original classification). **B**: Histogram of the mean values for each class.

Figure S1. Zero-primary control for the squid olfactory epithelium. **A:** A 50 µm thick section labeled with the anti-arginine antibody. **B:** A 50 µm section from the same slide as the section in A, except that the arginine primary antibody was omitted. Scale bar = 50 µm.

Figure S2. Mouse olfactory epithelium. **A-B:** RGB images of the mouse OE showing the Class 3 Bowman's glands (red AOIs) and Class 8 Ducts of the Bowman's glands (arrowhead). Purple AOIs are Class 7 SCs and basal cells. BL, basal lamina (dashed line); SC, sustentacular cell; OEC, olfactory ensheathing cell; BV, blood vessel. Scale bar = 10 µm.

Figure S3. Mouse vomeronasal organ. **A-B:** RGB images of the mouse VNO showing the Class 3 apical VNs (red AOIs), Class 7 rare VNs (purple AOI) and Class 9 ECs (orange AOIs). The remaining AOIs are color coded by class: 1, blue; 2, yellow; 4, green; 5, cyan; 10, cream. BL, basal lamina (dashed line); BV, blood vessel; EC, ensheathing cell; SC, sustentacular cell. Scale bar = 10 µm.

Figure S4. Zebrafish olfactory organ. **A-B:** RGB images of the zebrafish OE showing the Class 6 non-sensory cells (magenta AOIs), and Class 8 non-sensory cells (peach AOIs). The remaining AOIs are color coded by class: 1, blue; 2, yellow. BL; basal lamina (dashed lines); NSE, non-sensory epithelium. Scale bar = 10 µm.

Figure S5. Lobster olfactory (lateral) antennule. **A-B:** RGB images of the lobster olfactory antennule showing the Class 3 outer auxiliary cells (red AOIs). The remaining AOIs are color coded by class: 1, blue; 6, magenta. ATGs, aesthetasc tegumental glands; ACs, auxiliary cells. Scale bar = 10 µm.

Figure S6. Squid olfactory epithelium. **A-B:** RGB images of the squid OE showing the Class 2 glutamate and glutathione-negative type 2 ORNs (yellow AOIs), Class 7 glutamate-positive type 2 ORN (purple AOI) and Class 9 glutathione-positive type 3 and 5 cilia pockets (orange AOIs). The remaining AOIs are color coded by class: 1, blue; 4, green; 5, cyan; 6, magenta; 8, peach; 10, cream; 11, pink; 12, salmon. CP, cilia pocket; CT, connective tissue; BL, basal lamina (arrow). Scale bar = 10 µm.

UU IR Author Manuscript

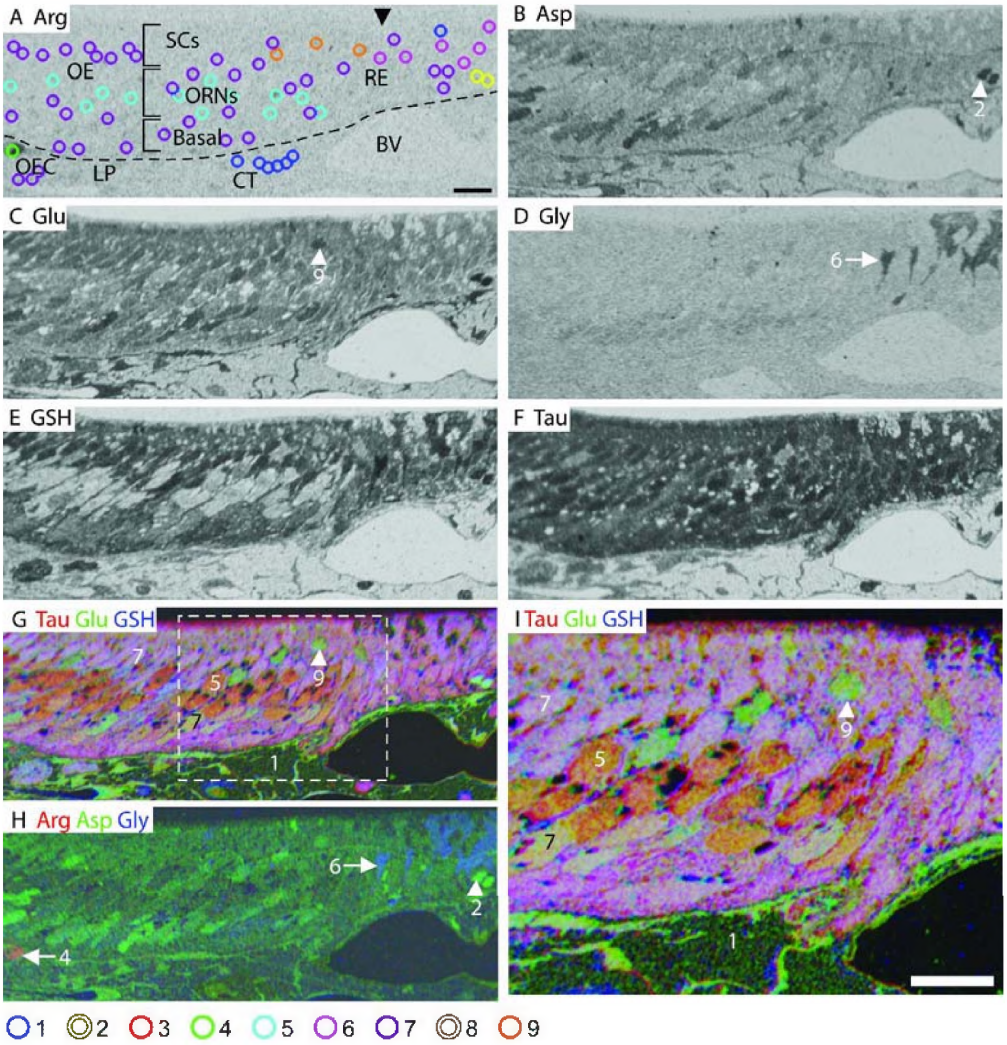

Figure 1. Mouse olfactory epithelium. A: Arginine (Arg). The image is marked to indicate the different layers of the olfactory epithelium (OE); arrowhead indicates the beginning of respiratory epithelium (RE). The AOI mask is overlaid and color coded by class (bottom): 1, blue; 2, yellow; 4, green; 5, cyan; 6, fuchsia; 7, purple; 9, orange (Classes 3 and 8 see Fig. S1). B: Aspartate (Asp). C: Glutamate (Glu). D: Glycine (Gly). E: GSH. F: Taurine (Tau). G: RGB image of Tau (red), Glu (green) and GSH (blue). H: RGB image of Arg (red), Asp (green), and Gly (blue). I: Higher magnification image of area within white dashed line in G. Numbers, arrows and arrowheads indicate the Class number. LP, lamina propria; SC, sustentacular cell; ORN, olfactory receptor neuron; OEC, olfactory ensheathing cell; CT, connective tissue; BV, blood vessel; dashed line in A indicates basal lamina. Scale bars = 10 μm.
211x221mm (300 x 300 DPI)

UU IR Author Manuscript

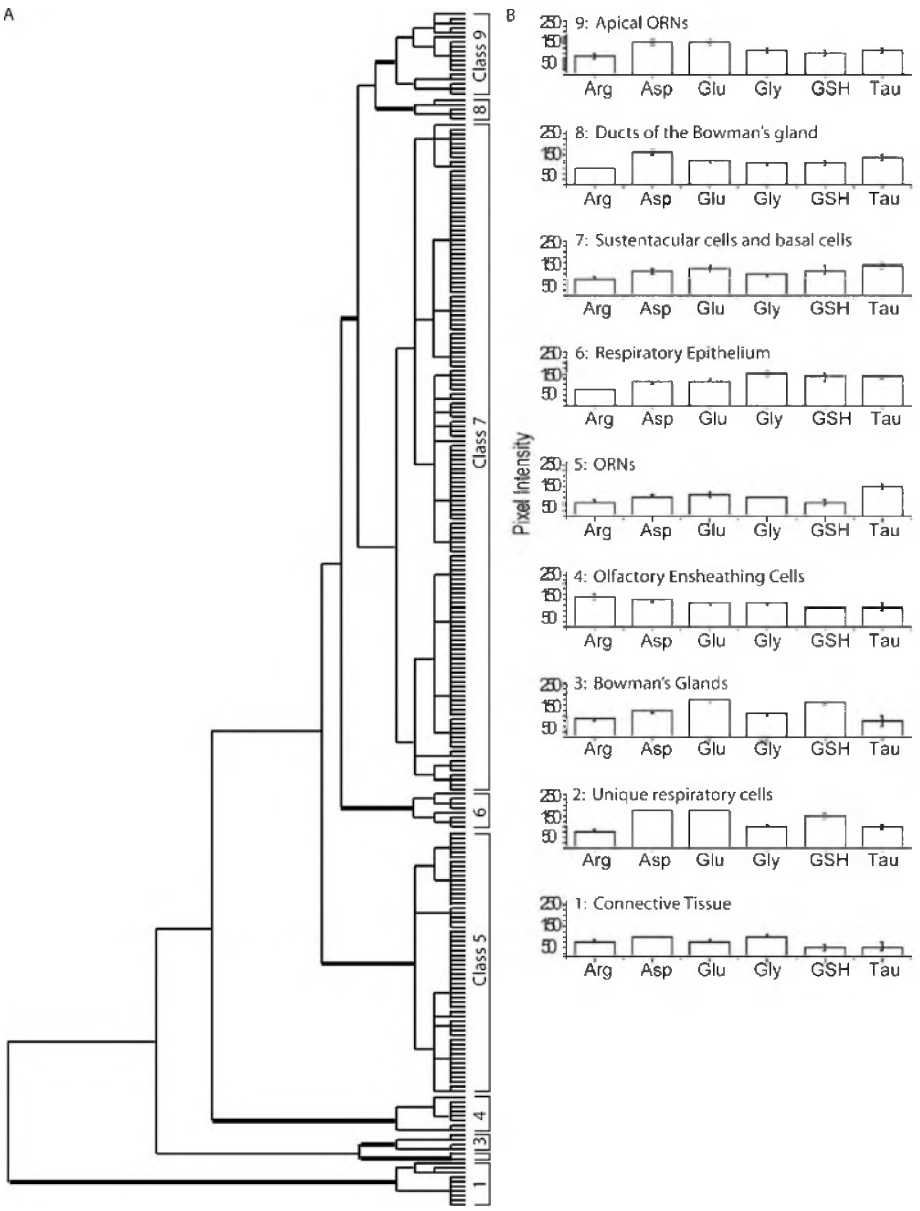

Figure 2. Hierarchical classification of AOIs from mouse olfactory epithelium. A: Dendrogram of the hierarchical cluster analysis. Statistical significance of each class determined using MANOVA. Thick bars correspond to class divisions. B: Histogram of the mean values for each class.
207x274mm (300 x 300 DPI)

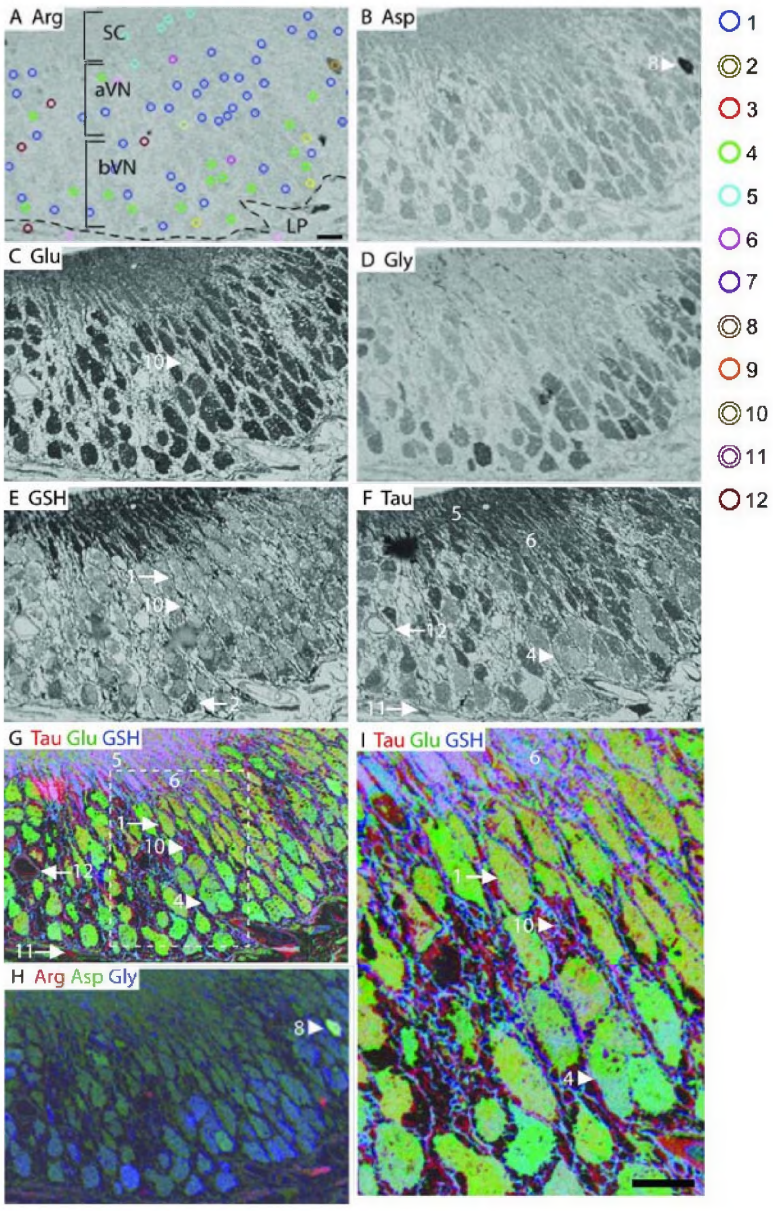

Figure 3. Mouse vomeronasal epithelium. A: Arginine. The image is marked to indicate the different layers of the OE. The AOI mask is overlaid and color coded by class (right): 1, blue; 2, yellow; 4, green; 5, cyan; 6, fuchsia; 8, peach; 10, cream; 11, pink; 12, maroon (Classes 3, 7 and 9 see Fig. S2). B: Aspartate. C: Glutamate. D: Glycine. E: GSH. F: Taurine. G-H: RGB images of the mouse VNO. I: Higher magnification image of area within white dashed line in G. Numbers, arrows and arrowheads indicate the Class number. aVN, apical vomeronasal neurons; bVN, basal vomeronasal neurons; LP, lamina propria; basal lamina, dashed line in A. Scale bars = 10 µm.
146x230mm (300 x 300 DPI)

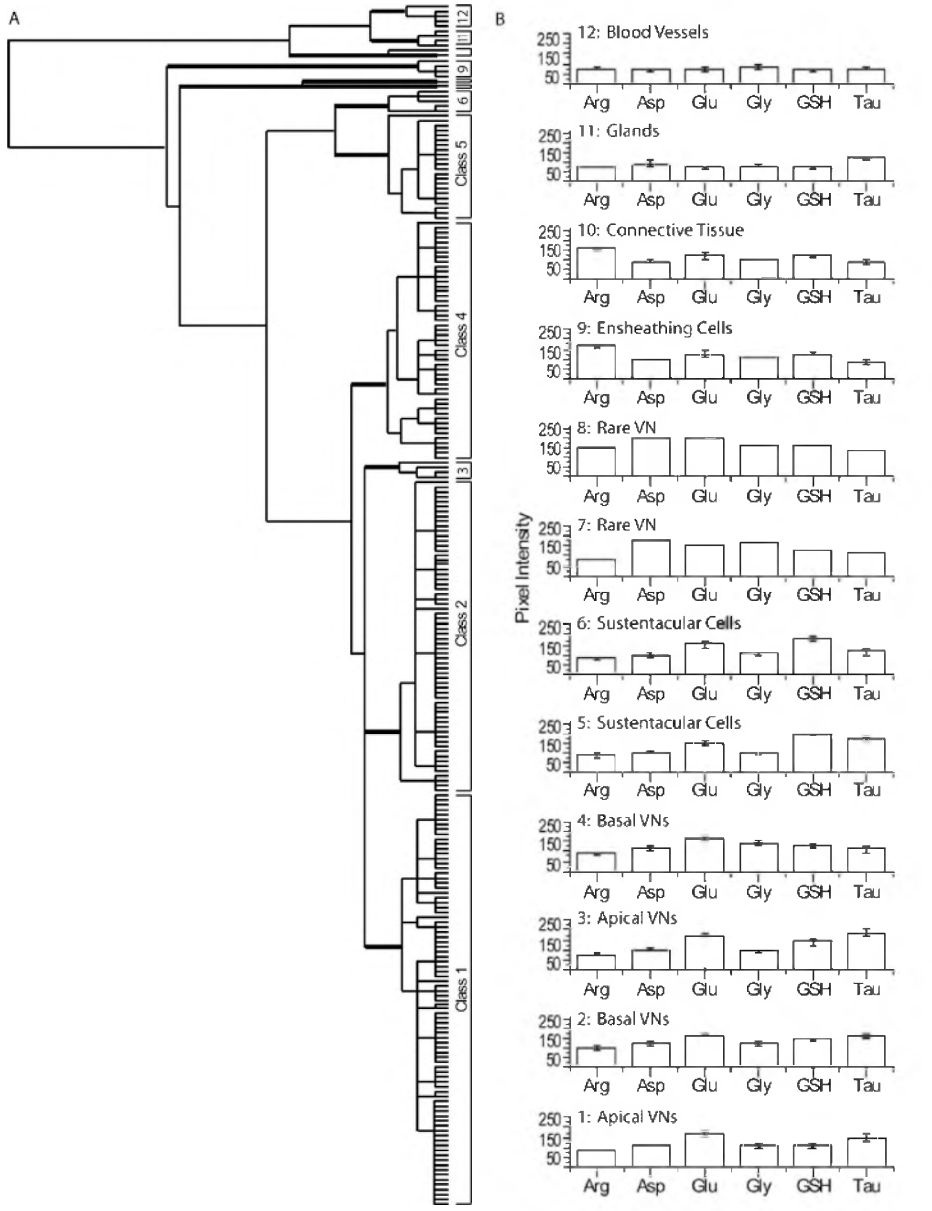

Figure 4. Hierarchical classification of AOIs from mouse vomeronasal epithelium. A: Dendrogram of the hierarchical cluster analysis. Statistical significance of each class determined using MANOVA. Thick bars correspond to class divisions. B: Histogram of the mean values for each class.
169x230mm (300 x 300 DPI)

UU IR Author Manuscript

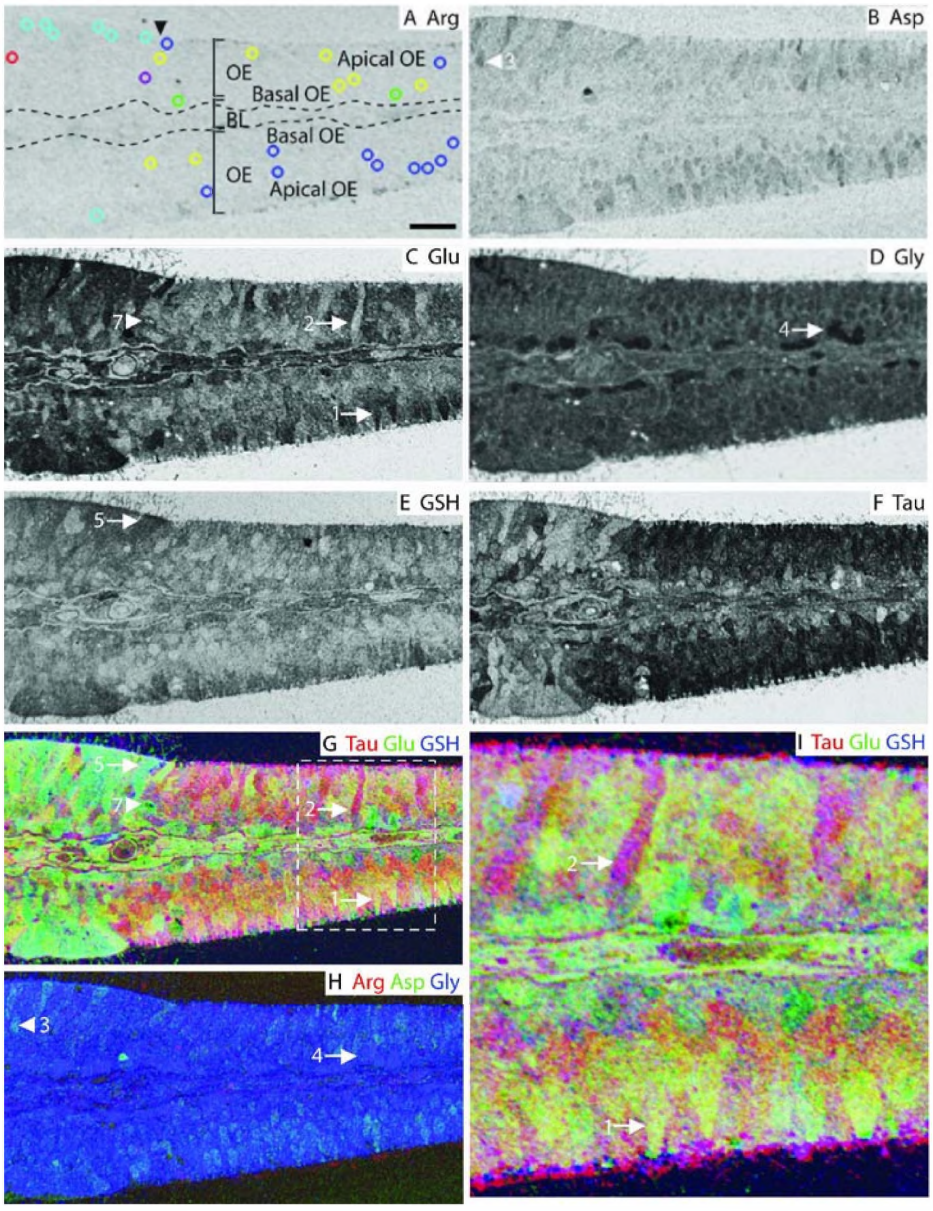

Figure 5. Zebrafish olfactory epithelium. A: Arginine. The image is marked to indicate the main features of the OE; arrowhead indicates the beginning of non-sensory epithelium. The AOI mask is overlaid and color-coded (see legend in Fig. 3) by class: 1, blue; 2, yellow; 3, red; 4, green; 5, cyan; 7, purple (Classes 6 and 8 see Fig. S3). B: Aspartate. C: Glutamate. D: Glycine. E: GSH. F: Taurine. G-H: RGB images of the zebrafish OE. I: Higher magnification image of area within white dashed line in G. Numbers, arrows and arrowheads indicate the Class number. BL, basal lamina (dashed line in A). Scale bars: A = 10 pm, I = 5 pm.

172x224mm (300 x 300 DPI)

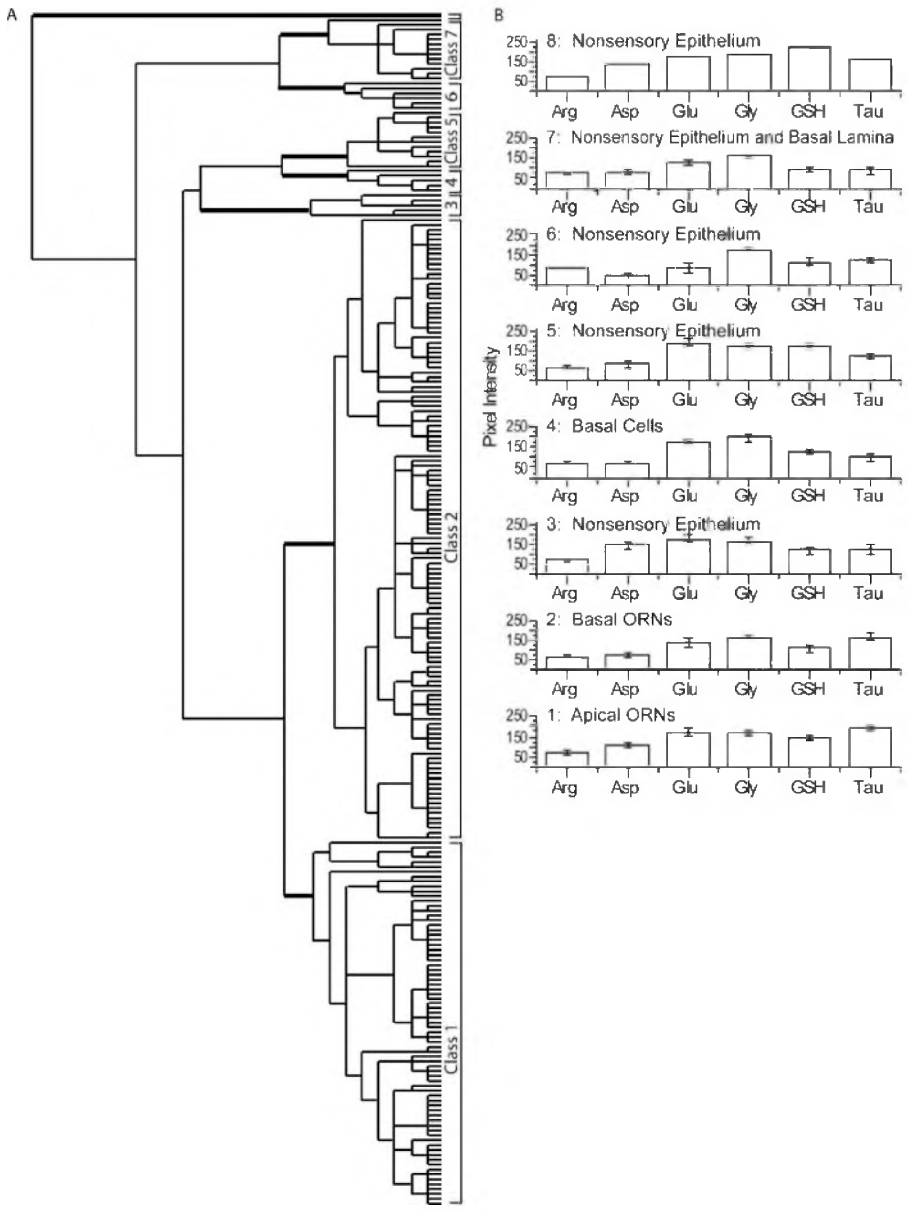

Figure 6. Hierarchical classification of AOIs from zebrafish olfactory epithelium. A: Dendrogram of the hierarchical cluster analysis. Statistical significance of each class determined using MANOVA. Thick bars correspond to class divisions. B: Histogram of the mean values for each class.
172x230mm (300 x 300 DPI)

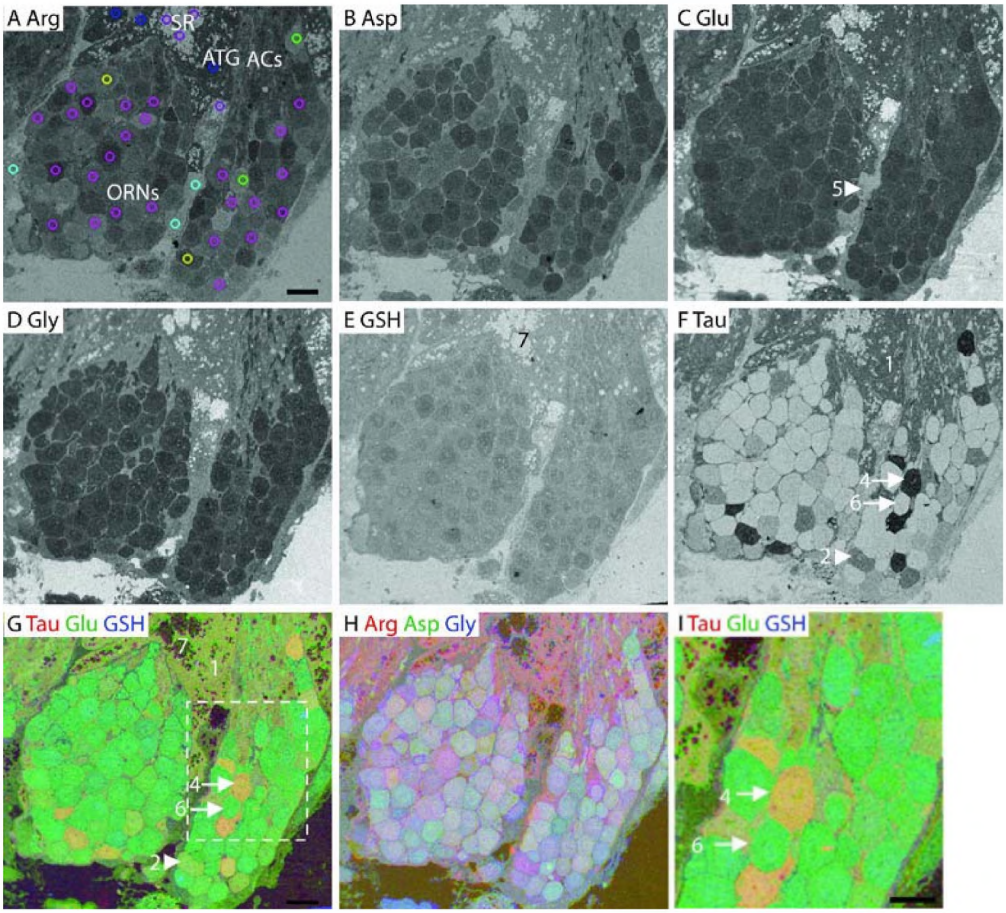

Figure 7. Lobster olfactory (lateral) antennule. A: Arginine. The image is marked to indicate the main features of the antennule. The AOI mask is overlaid and color-coded (see legend in Fig. 3) by class: 1, blue; 2, yellow; 4, green; 5, cyan; 6, fuchsia; 7, purple (Class 3 see Fig. S4). B: Aspartate. C: Glutamate. D: Glycine. E: GSH. F: Taurine. G-H: RGB images of the lobster olfactory antennule. I: Higher magnification image of area within white dashed line in G. Numbers, arrows and arrowheads indicate the Class number. ACs, auxiliary cells; ATG, aesthetasc tegumental gland; SR, secretory rosette. Scale bars = 10 µm.

212x192mm (300 x 300 DPI)

UU IR Author Manuscript

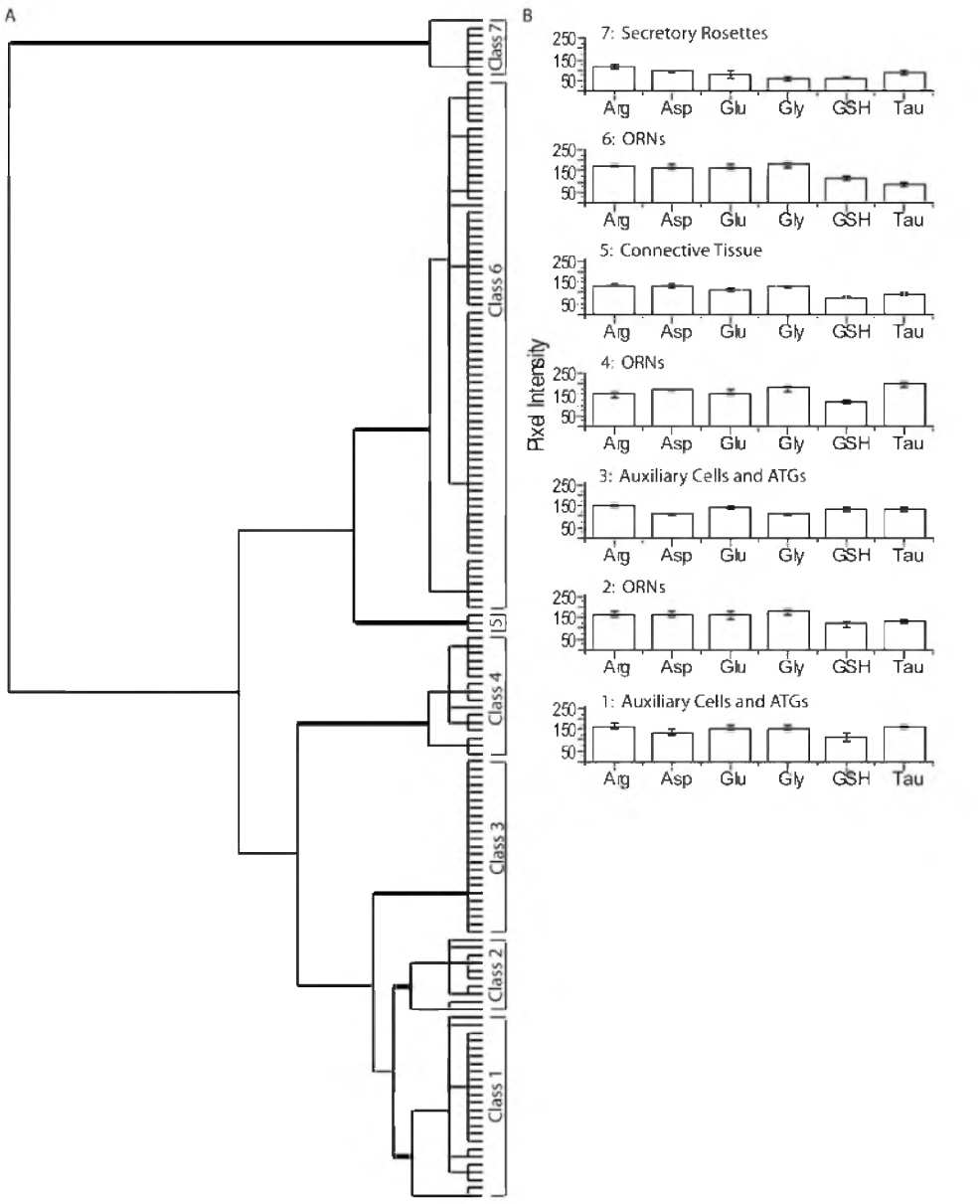

Figure 8. Hierarchical classification of AOIs from the lobster olfactory antennule. A: Dendrogram of the hierarchical cluster analysis. Statistical significance of each class determined using MANOVA. Thick bars correspond to class divisions. B: Histogram of the mean values for each class.
172x221mm (300 x 300 DPI)

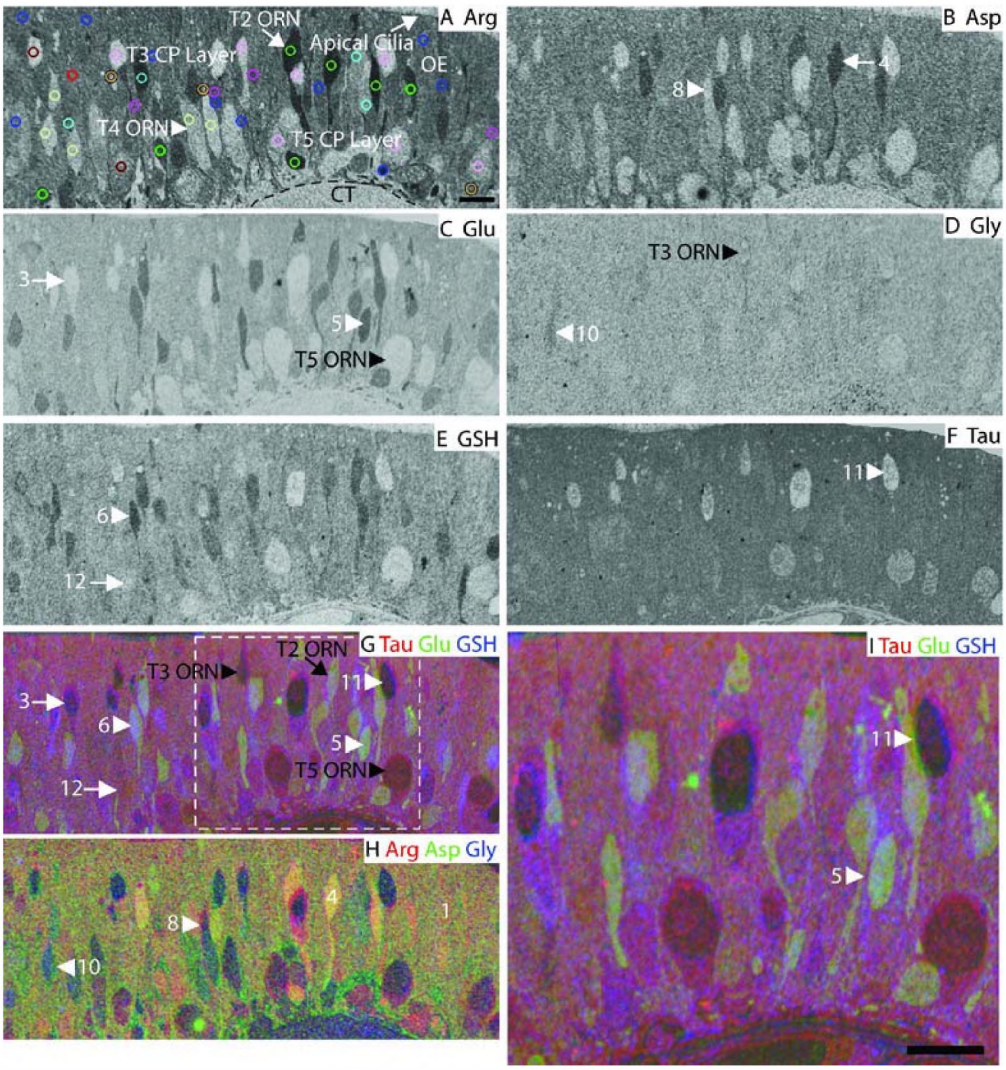

Figure 9. Squid olfactory epithelium. A: Arginine. The image is marked to indicate the main features of the OE. The AOI mask is overlaid and color-coded (see legend in Fig. 3) by class: 1, blue; 3, red; 4, green; 5, cyan; 6, fuchsia; 8, peach; 10, cream; 11, pink; 12, maroon (Classes 2, 7 and 9 see Fig. S5). B: Aspartate. C: Glutamate. D: Glycine. E: GSH. F: Taurine. G-H: RGB images of the squid OE. I: Higher magnification image of area within white dashed line in G. Numbers, arrows and arrowheads indicate the Class number. CP, cilia pocket; CT, connective tissue; T2, type 2 ORN; T3, type 3 ORN; T4, type 4 ORN; T5, type 5 ORN; basal lamina; dashed line in A. Scale bars = 10 µm.
172x183mm (300 x 300 DPI)

UU IR Author Manuscript

UU IR Author Manuscript

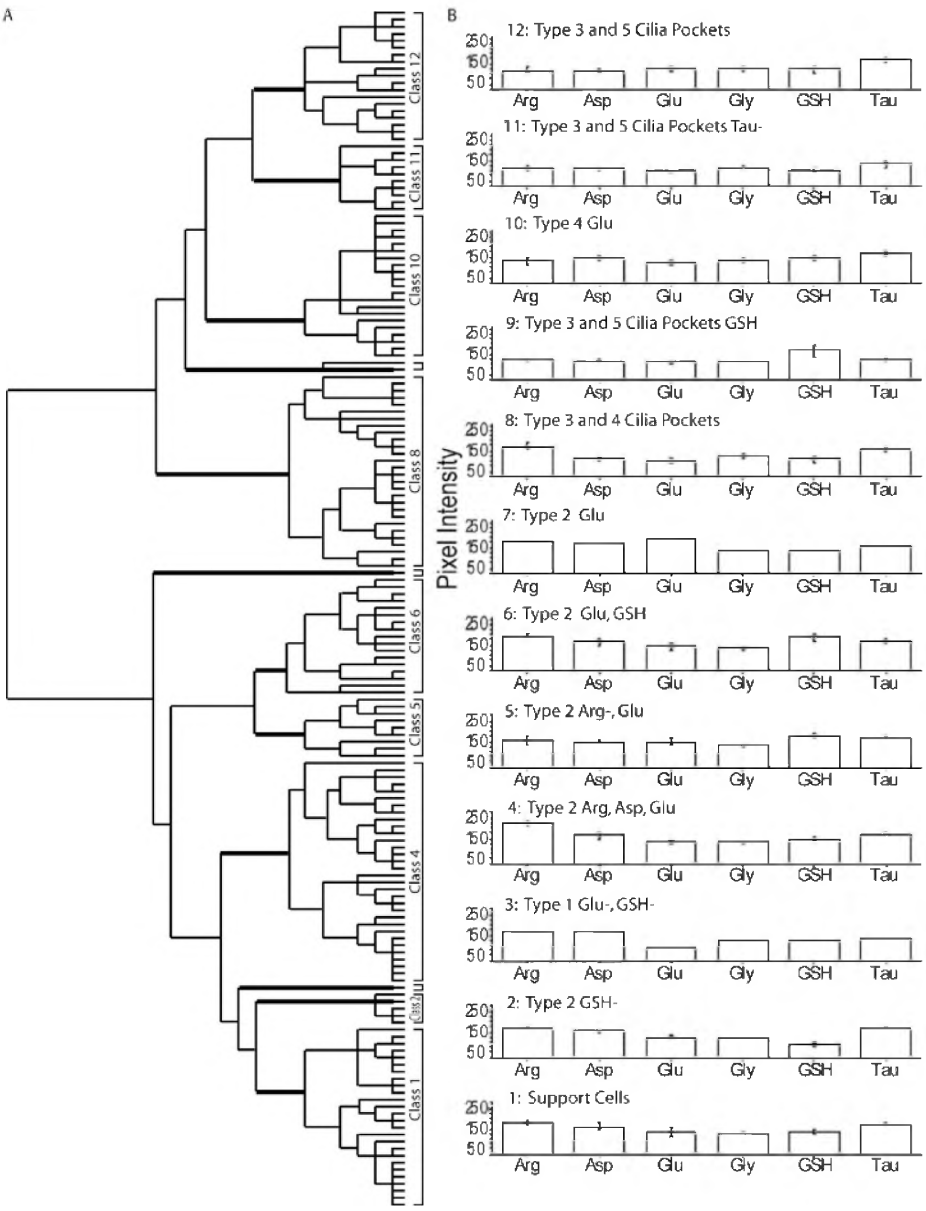

Figure 10. Hierarchical classification of AOIs from squid olfactory epithelium. A: Dendrogram of the hierarchical cluster analysis. Statistical significance of each class determined using MANOVA. Thick bars correspond to class divisions. B: Histogram of the mean values for each class.
172x225mm (300 x 300 DPI)

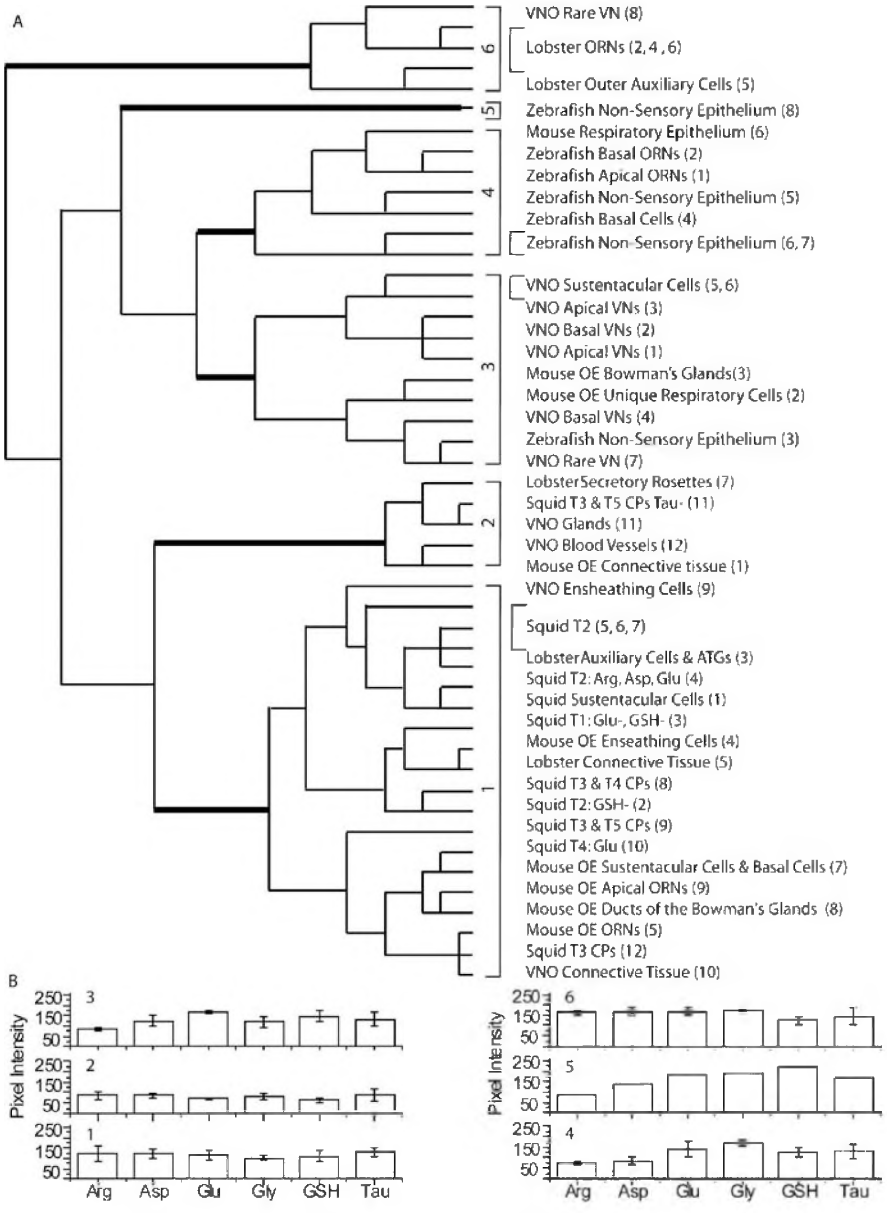

Figure 11. Hierarchical cluster analysis of the means from all the animal classes. A: Dendrogram of the hierarchical cluster analysis. Thick bars correspond to class divisions. Class descriptions are listed opposite each branch of the dendrogram (Class number from original classification). B: Histogram of the mean values for each class.
204x278mm (300 x 300 DPI)

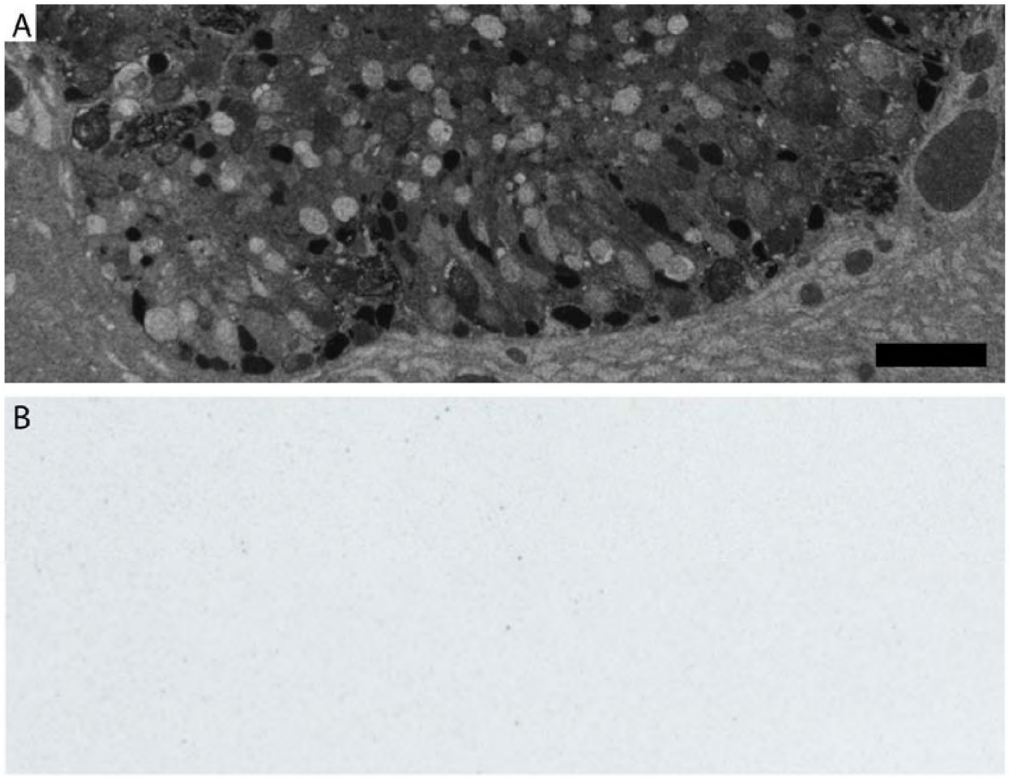

Figure S1. Zero-primary control for the squid olfactory epithelium. A: A 50 µm thick section labeled with the anti-arginine antibody. B: A 50 µm section from the same slide as the section in A, except that the arginine primary antibody was omitted. Scale bar = 50 µm.
144x110mm (300 x 300 DPI)

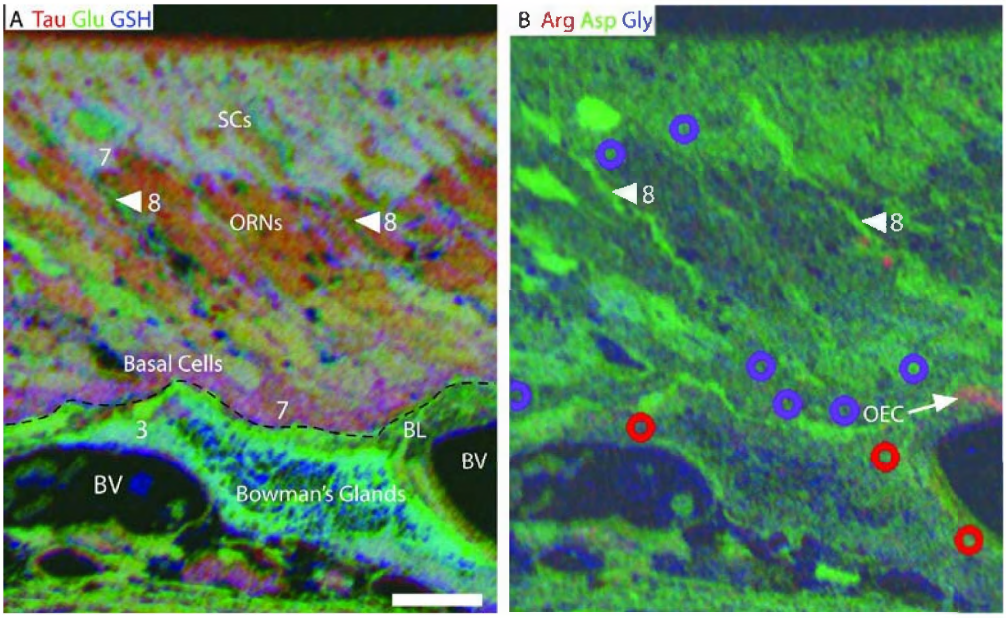

Figure S2. Mouse olfactory epithelium. A-B: RGB images of the mouse OE showing the Class 3 Bowman's glands (red AOIs) and Class 8 Ducts of the Bowman's glands (arrowhead). Purple AOIs are Class 7 SCs and basal cells. BL, basal lamina (dashed line); SC, sustentacular cell; OEC, olfactory ensheathing cell; BV, blood vessel. Scale bar = 10 µm.

211x128mm (300 x 300 DPI)

UU IR Author Manuscript

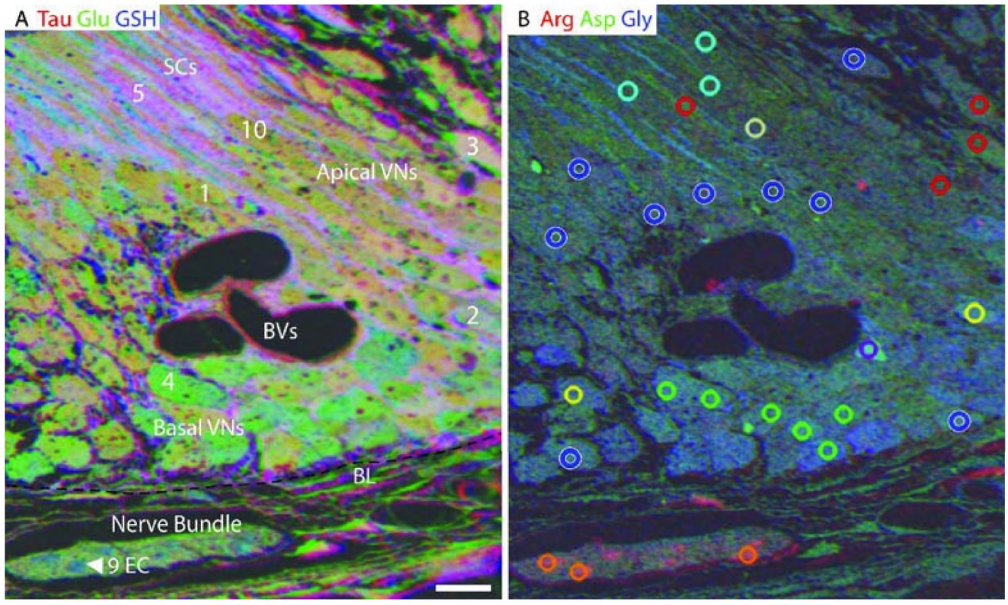

Figure S3. Mouse vomeronasal organ. A-B: RGB images of the mouse VNO showing the Class 3 apical VNs (red AOIs), Class 7 rare VNs (purple AOI) and Class 9 ECs (orange AOIs). The remaining AOIs are color coded by class: 1, blue; 2, yellow; 4, green; 5, cyan; 10, cream. BL, basal lamina (dashed line); BV, blood vessel; EC, ensheathing cell; SC, sustentacular cell. Scale bar = 10 µm.
212x125mm (300 x 300 DPI)

UU IR Author Manuscript

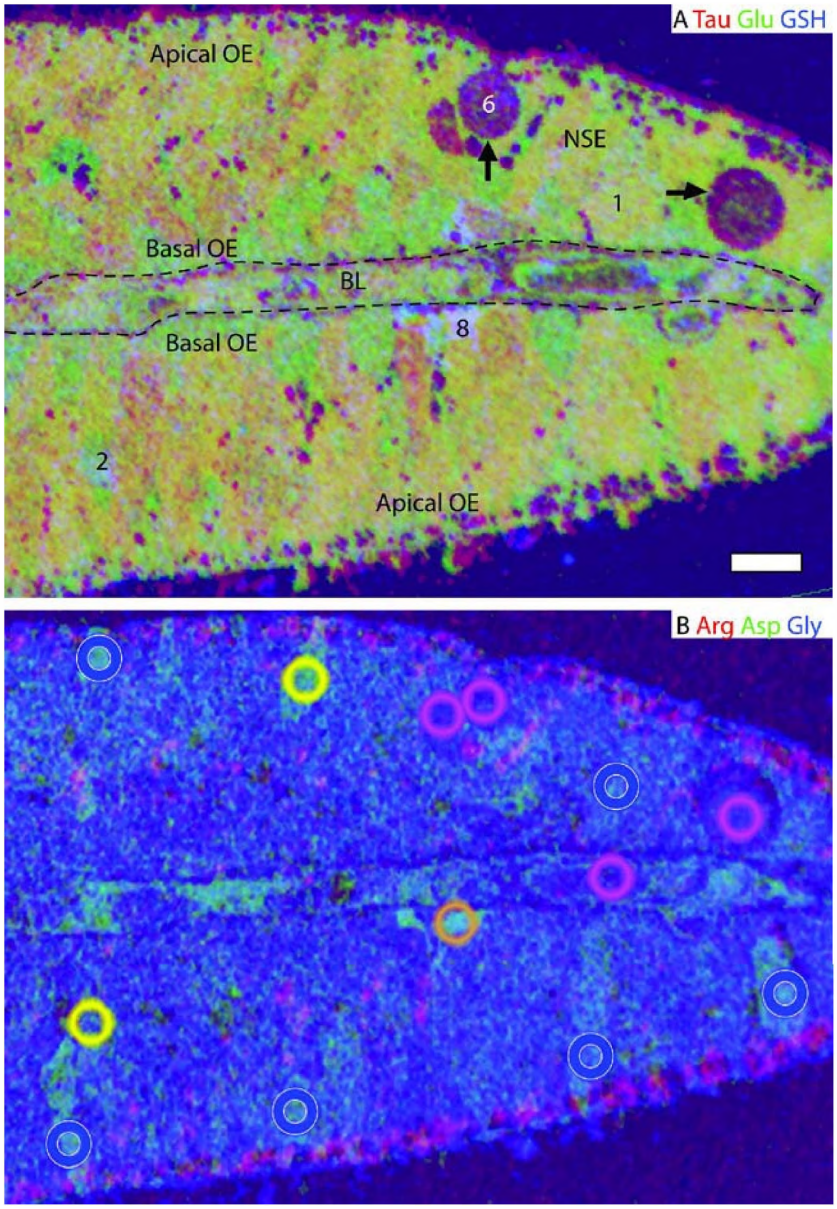

Figure S4. Zebrafish olfactory organ. A-B: RGB images of the zebrafish OE showing the Class 6 non-sensory cells (magenta AOIs), and Class 8 non-sensory cells (peach AOIs). The remaining AOIs are color coded by class: 1, blue; 2, yellow. BL; basal lamina (dashed lines); NSE, non-sensory epithelium. Scale bar = 10 µm.
156x226mm (300 x 300 DPI)

UU IR Author Manuscript

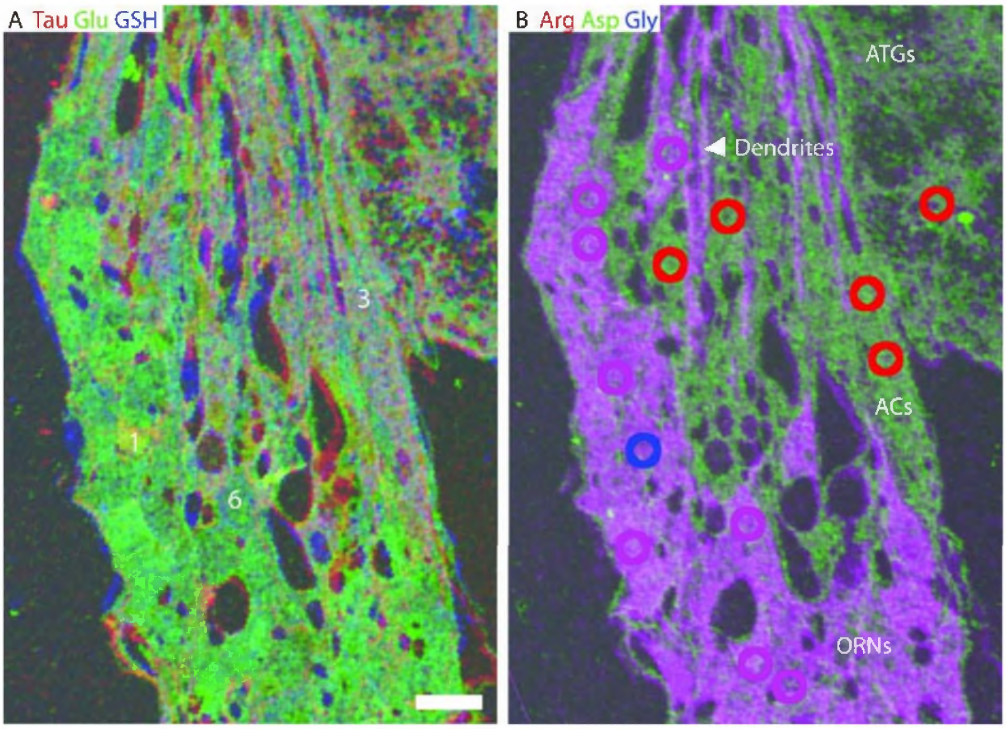

Figure S5. Lobster olfactory (lateral) antennule. A-B: RGB images of the lobster olfactory antennule showing the Class 3 outer auxiliary cells (red AOIs). The remaining AOIs are color coded by class: 1, blue; 6, magenta. ATGs, aesthetasc tegumental glands; ACs, auxiliary cells. Scale bar = 10 µm.
200x144mm (300 x 300 DPI)

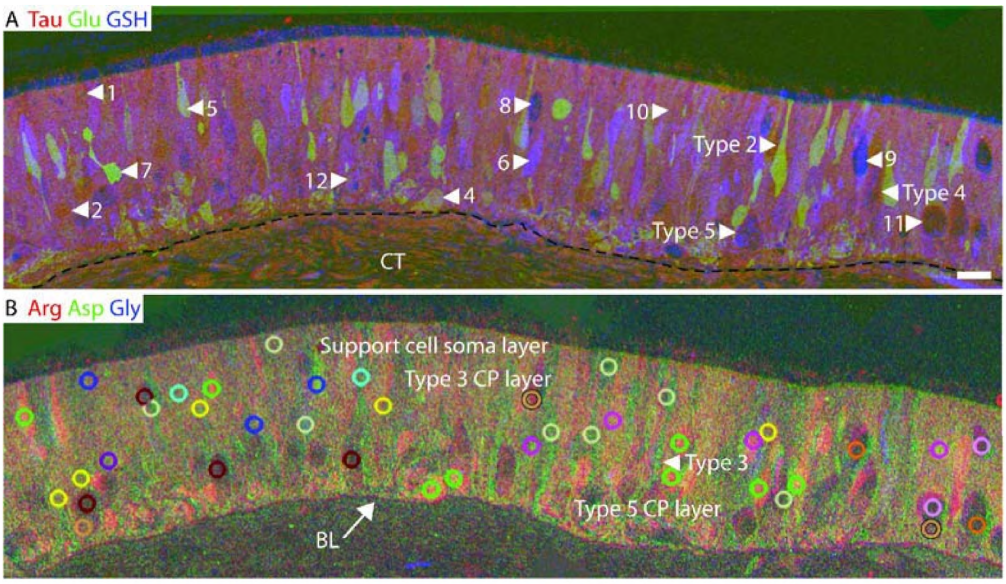

Figure S6. Squid olfactory epithelium. A-B: RGB images of the squid OE showing the Class 2 glutamate and glutathione-negative type 2 ORNs (yellow AOIs), Class 7 glutamate-positive type 2 ORN (purple AOI) and Class 9 glutathione-positive type 3 and 5 cilia pockets (orange AOIs). The remaining AOIs are color coded by class: 1, blue; 4, green; 5, cyan; 6, magenta; 8, peach; 10, cream; 11, pink; 12, salmon. CP, cilia pocket; CT, connective tissue; BL, basal lamina (arrow). Scale bar = 10 µm.
210x120mm (300 x 300 DPI)

UU IR Author Manuscript